Reduction of serum Pai-1 levels and liver Pai-1 mRNA levels in Min mice by Pai-1 inhibitors

It has been recognized that Pai-1 inhibitors, SK-216 and SK-116, inhibit Pai-1 activity. The present study revealed that Pai-1 inhibitors suppress Pai-1 at both protein and mRNA levels. The highest dose used in this study, 100 p.p.m. SK-216, suppressed serum Pai-1 levels to the wild-type level (Figure 2A). Real-time PCR revealed that administration of 25, 50 and 100 p.p.m. SK-216 for 9 weeks suppressed increased hepatic Pai-1 mRNA levels (Figure 2B) in Min mice in a dose-dependent manner. Another Pai-1 inhibitor, SK-116, also reduced serum Pai-1 level in Min mice from 20.1 ± 6.7 ng/ml (0 p.p.m.) to 6.9 ± 4.1 ng/ml (50 p.p.m.). In the immunohistochemistry study, Pai-1 could be detected more weakly in non-tumorous and polyp epithelial cells of the small intestine in Min mice treated with 100 p.p.m. SK-216 compared with that of untreated Min mice (data not shown).

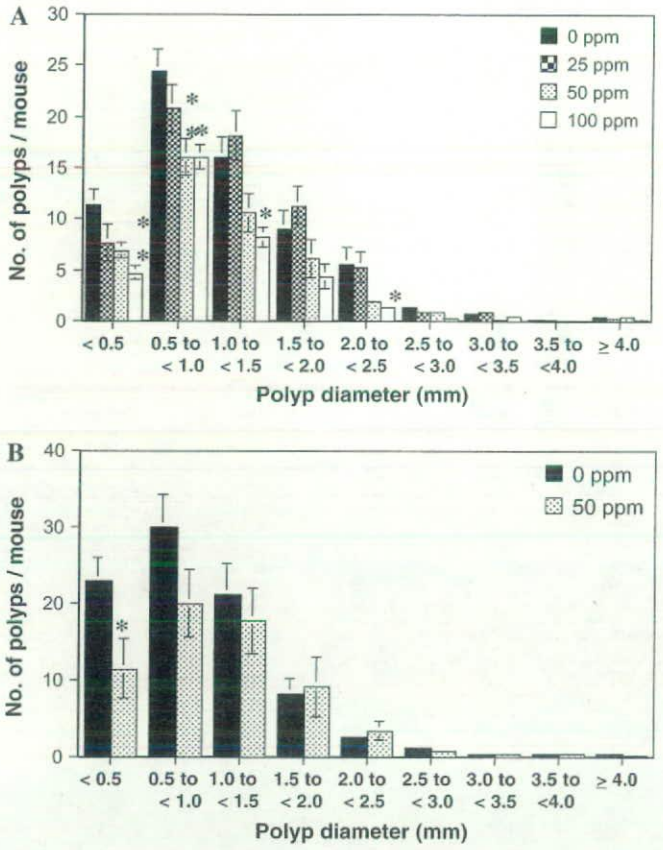

Fig. 3. Effects of SK-216 and SK-116 on the size distribution of intestinal polyps in Min mice. (**A**) Min mice were fed a basal diet (black filled box) or a diet containing 25 p.p.m. (large dotted box), 50 p.p.m. (dotted box) or 100 p.p.m. (open box) SK-216 for 9 weeks. (**B**) Min mice were fed a basal diet (black filled box) or a diet containing 50 p.p.m. (dotted box) SK-116 for 9 weeks. The number of polyps per mouse in each size class is given as a mean ± standard error. $^{*}P < 0.05$; $^{**}P < 0.01$.

Improvement of serum lipid levels in Min mice by Pai-1 inhibitors

Consistent with our previous reports (6–8), serum TG levels in the Min mice fed the basal diet at 15 weeks of age were higher at 117 mg/dl than the 39.2 mg/dl in wild-type mice (Figure 4). Total cholesterol levels in Min mice were also increased 1.3-fold (92 versus 62 mg/dl) while free fatty acid levels were almost the same in both Min and wild-type mice. Administration of 50 and 100 p.p.m. SK-216 decreased serum levels of TG in Min mice to 74 and 57% of the untreated control value, respectively (Figure 4). Administration of 50 and 100 p.p.m. SK-216 also decreased serum levels of TG in wild-type mice from 39.2 to 18.4 and 17.6 mg/dl ($P < 0.01$), respectively. The levels of total cholesterol and free fatty acid were not decreased by SK-216 treatment.

Reduction in serum TG levels was also observed in the 50 p.p.m. SK-116-treated group. Administration of 50 p.p.m. SK-116 decreased serum levels of TG in Min mice to 76% of the untreated control value.

Decrease of Pai-1 mRNA levels and NFκB binding activity in intestinal mucosa cells by Pai-1 inhibitor

To investigate whether the Pai-1 inhibitors directly targeted the intestinal mucosa, SK-216 in diet was administered to C57/BL6 mice. As shown in Figure 5A, treatment with soy oil, consisting of TG as a major component, increased Pai-1 expression levels in the intestinal mucosa of two out of three mice. A weeklong treatment with 100 p.p.m. SK-216 reduced Pai-1 mRNA levels to lower than non-treated mice in two out of three mice. Similar results were obtained in an *in vitro* study. Treatment with 50 μM SK-216 for 17 h reduced basal Pai-1 protein levels in the colon cancer cell line RCN-9 (Figure 5B). Moreover, 50 μM SK-216 treatment for 6 h decreased NFκB activity (Figure 5C). These results suggest that decreased NFκB activity may be involved in both suppression of Pai-1 mRNA and inhibition of polyp formation in Min mice by SK-216 treatment.

Discussion

This study provided evidence that administration of the PAI-1 inhibitors SK-216 and SK116, which also reduce Pai-1 mRNA and protein levels, suppresses intestinal polyp formation in Min mice. It is therefore speculated that Pai-1 activity itself may play an important role in intestinal polyp formation in *Apc*-deficient mice.

We previously reported markedly increased serum levels of TGs and low levels of LPL mRNA in liver and small intestine in Min mice compared with their wild-type counterparts (6–8). Thus, we hypothesized that hypertriglyceridemia is a leading cause of intestinal polyp

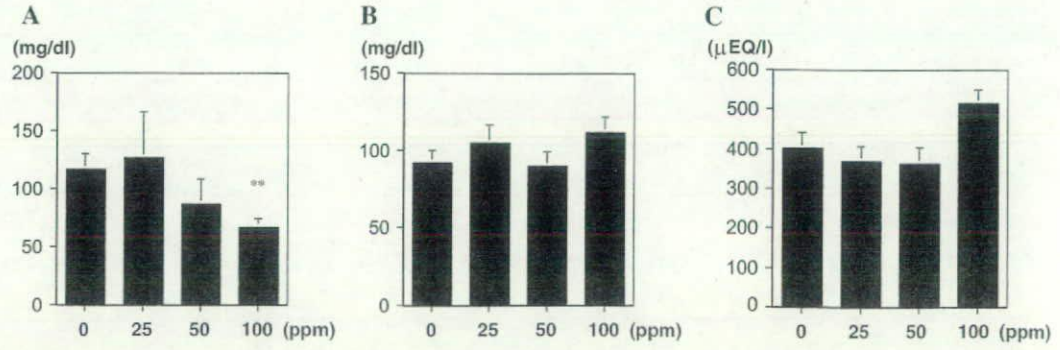

Fig. 4. Suppression of serum lipid levels in Min mice by SK-216. Values for serum levels of TG (**A**), total cholesterol (**B**) and free fatty acids (**C**) in Min mice given diet containing SK-216 at doses of 25–100 p.p.m. for 9 weeks are shown. Data are means ± standard errors. $^{**}P < 0.01$.

formation. However, the molecular mechanisms could only be partially addressed since only little information is available as to effects of TG-rich lipoproteins (23,24). TG-rich lipoproteins from type IV hyperlipidemic patients induce phosphorylation of p38 mitogen-activated protein kinase, and CAMP response element binding protein Inhibitor of kappa B α and activate DNA-binding activity of transcriptional factors, CREB, NFκB and AP-1. TG-rich lipoproteins also upregulate the expression of proinflammatory and adhesion-related genes, monocyte chemoattractant protein-1, interleukin-6, intercellular adhesion molecule-1, vascular cell adhesion molecule-1 and PAI-1. These mitogen-activated protein kinase pathways and molecules are well known to be involved in endothelial cell growth. Treatment of smooth muscle cells with low-density lipoprotein results in the activation of protein kinase C and mitogen-activated protein kinase as well as induction of the cell cycle-related genes c-*fos*, c-*myc* (24) and early growth response gene-1 (*egr*-1, 25). Thus, hypertriglyceridemia may also modify epithelial cell growth. To explore molecular mechanisms underlying the link between hypertriglyceridemia and polyp formation, we first selected candidate molecules from those which are increased with the metabolic syndrome (26). Focusing on adipocytokines, we selected Pai-1 among possible candidate molecules, including adiponectin, IL-1, IL-6, leptin and tumor necrosis factor α. Liver was used for the RT–PCR analysis because this is the major Pai-1-producing organ and expression may correlate with hyperlipidemic states in the mice. Moreover, Pai-1 immunostaining was strong in small intestinal epithelial cells of Min mice. The reason why PAI-1 inhibitors also reduced serum TG levels remains unclear and examination of Pai-1 effects on TG metabolism would appear warranted.

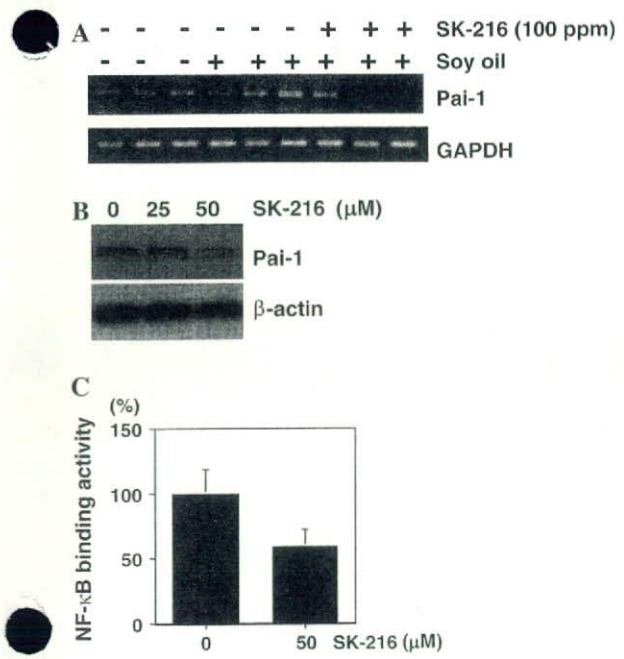

Fig. 5. Decrease of Pai-1 mRNA levels and NFκB-binding activity in intestinal mucosa/RCN-9 cells by SK-216 treatment. (**A**) RT–PCR for Pai-1 and GAPDH are shown. C57/BL mice ($n = 3$ for each group) were fed diet with or without 100 p.p.m. SK-216 for a week and gavaged with 200 μl soy oil 2 h before collecting intestinal mucosa. RT–PCR was performed as describe in Materials and Methods. (**B**) Western blotting for Pai-1 and beta-actin are shown. RCN-9 cells grown in 24-well plates were treated for 17 h with indicated doses of SK-216. Actin was used as a loading control. (**C**) RCN-9 cells grown in six-well plates were treated with and without 50 μM SK-216 for 6 h. Nuclear fractions of RCN-9 cells were isolated and analyzed for NFκB-binding activity as describe in Materials and Methods. Values represent means ± standard errors of three wells.

Regarding the mechanisms underlying suppression of intestinal polyp formation by PAI-1 inhibitor in Min mice, contrary reports should be noted (10,27). Inhibition of PAI-1 activation results in generation of active growth factors from inactivated forms like heparin-bound epidermal growth factor, hepatocyte growth factor, basic fibroblast growth factor or insulin-like growth factors (10). Moreover, suppression of PAI-1 enhances growth factor signaling through the phosphatidylinositol 3-kinase–protein kinase B route (27). These reports indicate that PAI-1 may inhibit cell proliferation. However, Li *et al.* (28) have reported that genetic Pai-1 deficiency reduced the number of aggressive fibromatosis tumors in Apc/Apc1638N mice. The data from Li *et al.* were partially consistent with our results. Especially in male Pai-1-null Apc/Apc1638N mice, the number of aggressive fibromatosis tumors was decreased. However, no significant difference was observed in the number of gastrointestinal tumors compared with that of Apc/Apc1638N mice (0.7 ± 0.5 versus 1.1 ± 0.4; $P > 0.05$). These results may be due to weak statistical power derived from the relatively few intestinal polyps that developed in Apc/Apc1638N mice. Pai-1$^{-/-}$ tumor cells demonstrated reduced proliferation and motility *in vitro* (28). In addition, our *in vitro* study demonstrated that Pai-1 inhibitor SK-216 also decreased NFκB activity. This decrease in NFκB activity may be involved in both suppression of Pai-1 levels and inhibition of polyp development in Min mice.

In conclusion, this study indicated that the PAI-1 inhibitors, SK-216 and SK-116, have potential benefit for suppression of intestinal polyp development. Thus, SK-216, SK-116 and related derivatives could be promising candidate chemopreventive agents for colon cancer. As it is becoming increasingly clear that hyperlipidemia is an important player in carcinogenesis, our observations may lead to a better understanding of the role of hyperlipidemia in colon carcinogenesis.

Funding

Grants-in-Aid for Cancer Research, for the Third-Term Comprehensive 10-Year Strategy for Cancer Control from the Ministry of Health, Labour, and Welfare of Japan (H19-013).

Acknowledgements

During the performance of this work, N.N. was the recipient of a Research Resident fellowship from the Foundation for Promotion of Cancer Research.

Conflict of Interest Statement: None declared.

Table II. Suppression of intestinal polyp development in Min mice by SK-116

No. of polyps/mouse		Small intestine			Colon	Total
Group (p.p.m.)	No. of mice	Proximal	Middle	Distal		
0	10	4.8 ± 0.6[a]	23.4 ± 3.1	58.7 ± 7.2	1.9 ± 0.5	88.8 ± 10.3
50	10	2.0 ± 0.4[b] (42)[c]	16.2 ± 2.9 (69)	42.9 ± 7.2 (73)	1.0 ± 0.3	62.1 ± 9.5 (70)

[a]Data are means ± standard errors.
[b]Significantly different from the basal diet group at $P < 0.01$.
[c]Numbers in parentheses are percentages of the control basal diet values.

References

1. Le Marchand,L. *et al.* (1997) Associations of sedentary lifestyle, obesity, smoking, alcohol use, and diabetes with the risk of colorectal cancer. *Cancer Res.*, **57**, 4787–4794.
2. Abu-Abid,S. *et al.* (2002) Obesity and cancer. *J. Med.*, **33**, 73–86.
3. Yamada,K. *et al.* (1998) Relation of serum total cholesterol, serum triglycerides and fasting plasma glucose to colorectal carcinoma *in situ*. *Int. J. Epidemiol.*, **27**, 794–798.
4. Kaye,J.A. *et al.* (2002) Statin use, hyperlipidaemia, and the risk of breast cancer. *Br. J. Cancer*, **86**, 1436–1439.
5. Otani,T. *et al.* (2006) Serum triglycerides and colorectal adenoma in a case-control study among cancer screening examinees (Japan). *Cancer Causes Control*, **17**, 1245–1252.
6. Niho,N. *et al.* (2003) Concomitant suppression of hyperlipidemia and intestinal polyp formation in *Apc*-deficient mice by peroxisome proliferator-activated receptor ligands. *Cancer Res.*, **63**, 6090–6095.
7. Niho,N. *et al.* (2003) Dose-dependent suppression of hyperlipidemia and intestinal polyp formation in Min mice by pioglitazone, a PPAR gamma ligand. *Cancer Sci.*, **94**, 960–964.
8. Niho,N. *et al.* (2005) Concurrent suppression of hyperlipidemia and intestinal polyp formation by NO-1886, increasing lipoprotein lipase activity in Min mice. *Proc. Natl Acad. Sci. USA*, **102**, 2970–2974.
9. Luchtenborg,M. *et al.* (2004) *APC* mutations in sporadic colorectal carcinomas from The Netherlands Cohort Study. *Carcinogenesis*, **25**, 1219–1226.
10. Kortlever,R.M. *et al.* (2006) Rapid uptake of tyrphostin into A431 human epidermoid cells is followed by delayed inhibition of epidermal growth factor (EGF)-stimulated EGF receptor tyrosine kinase activity. *Cell Cycle*, **5**, 2697–2703.
11. Nilsson,L. *et al.* (1998) Unsaturated fatty acids increase plasminogen activator inhibitor-1 expression in endothelial cells. *Arterioscler. Thromb. Vasc. Biol.*, **18**, 1679–1685.
12. Ferran,C. *et al.* (1995) Inhibition of NF-kappa B by pyrrolidine dithiocarbamate blocks endothelial cell activation. *Biochem. Biophys. Res. Commun.*, **214**, 212–223.
13. Eriksson,P. *et al.* (1998) Very-low-density lipoprotein response element in the promoter region of the human plasminogen activator inhibitor-1 gene implicated in the impaired fibrinolysis of hypertriglyceridemia. *Arterioscler. Thromb. Vasc. Biol.*, **18**, 20–26.
14. Barbareschi,M. *et al.* (1995) Novel methods for the determination of the angiogenic activity of human tumors. *Breast Cancer Res. Treat.*, **36**, 181–192.
15. Bajou,K. *et al.* (2002) Human breast adenocarcinoma cell lines promote angiogenesis by providing cells with uPA-PAI-1 and by enhancing their expression. *Int. J. Cancer*, **100**, 501–506.
16. Sier,C.F. *et al.* (1994) Inactive urokinase and increased levels of its inhibitor type 1 in colorectal cancer liver metastasis. *Gastroenterology*, **107**, 1449–1456.
17. Bajou,K. *et al.* (1998) Absence of host plasminogen activator inhibitor 1 prevents cancer invasion and vascularization. *Nat. Med.*, **4**, 923–928.
18. Sier,C.F. *et al.* (1991) Imbalance of plasminogen activators and their inhibitors in human colorectal neoplasia. Implications of urokinase in colorectal carcinogenesis. *Gastroenterology*, **101**, 1522–1528.
19. Li,C.F. *et al.* (2006) An association between the 4G polymorphism in the PAI-1 promoter and the development of aggressive fibromatosis (desmoid tumor) in familial adenomatous polyposis patients. *Fam. Cancer*, **6**, 89–95.
20. Moser,A.R. *et al.* (1990) A dominant mutation that predisposes to multiple intestinal neoplasia in the mouse. *Science*, **247**, 322–324.
21. Charlton,P.A. *et al.* (1996) Evaluation of a low molecular weight modulator of human plasminogen activator inhibitor-1 activity. *Thromb. Haemost.*, **75**, 808–815.
22. Ploplis,V.A. *et al.* (2004) Enhanced *in vitro* proliferation of aortic endothelial cells from plasminogen activator inhibitor-1-deficient mice. *J. Biol. Chem.*, **279**, 6143–6151.
23. Jiang,T. *et al.* (2005) Diet-induced obesity in C57BL/6J mice causes increased renal lipid accumulation and glomerulosclerosis via a sterol regulatory element-binding protein-1c-dependent pathway. *J. Biol. Chem.*, **280**, 32317–32325.
24. Norata,G.D. *et al.* (2007) Post-prandial endothelial dysfunction in hypertriglyceridemic subjects: molecular mechanisms and gene expression studies. *Atherosclerosis*, **193**, 321–327.
25. Sachinidis,A. *et al.* (1993) Lipoproteins induce expression of the early growth response gene-1 in vascular smooth muscle cells from rat. *Biochem. Biophys. Res. Commun.*, **192**, 794–799.
26. Bahia,L. *et al.* (2006) Relationship between adipokines, inflammation, and vascular reactivity in lean controls and obese subjects with metabolic syndrome. *Clinics*, **61**, 433–440.
27. Kortlever,R.M. *et al.* (2006) Plasminogen activator inhibitor-1 is a critical downstream target of p53 in the induction of replicative senescence. *Nat. Cell Biol.*, **8**, 877–884.
28. Li,C.F. *et al.* (2005) Plasminogen activator inhibitor-1 (PAI-1) modifies the formation of aggressive fibromatosis (desmoid tumor). *Oncogene*, **24**, 1615–1624.

Received August 10, 2007; revised January 23, 2008; accepted January 23, 2008

Carcinogenesis vol.29 no.8 pp.1608–1613, 2008
doi:10.1093/carcin/bgn152
Advance Access publication June 20, 2008

Increased expression of inducible nitric oxide synthase (iNOS) in *N*-nitrosobis(2-oxopropyl)amine-induced hamster pancreatic carcinogenesis and prevention of cancer development by ONO-1714, an iNOS inhibitor

Mami Takahashi[1,*], Tsukasa Kitahashi[1], Rikako Ishigamori[1], Michihiro Mutoh[1], Masami Komiya[1], Hidetaka Sato[2], Yoshihisa Kamanaka[3], Masao Naka[3], Takayuki Maruyama[3], Takashi Sugimura[1] and Keiji Wakabayashi[1]

[1]Cancer Prevention Basic Research Project, National Cancer Center Research Institute, 1-1 Tsukiji 5-chome, Chuo-ku, Tokyo 104-0045, Japan, [2]Japan Food Research Laboratories, Bunkyo 2-3, Chitose-shi, Hokkaido 066-0052, Japan and [3]Minase Research Institute, Ono Pharmaceutical Co. Ltd., 1-1, Sakurai 3-chome, Shimamoto-cho, Mishima-gunn, Osaka 618-8585, Japan

*To whom correspondence should be addressed. Tel: +81 3 3542 2511; Fax: +81 3 3543 9305;
Email: mtakahas@ncc.go.jp

Elevated protein expression of inducible nitric oxide synthase (iNOS) has been observed in human pancreatic cancers and therefore iNOS may play important roles in pancreatic carcinogenesis. This was examined in the present study, using an experimental model with *N*-nitrosobis(2-oxopropyl)amine (BOP)-treated hamsters. Reverse transcription–polymerase chain reaction analysis demonstrated iNOS expression in a hamster pancreatic cancer cell line as well as in human pancreatic cancer cell lines. Immunohistochemical analysis revealed increased expression of iNOS protein in atypical hyperplasia and ductal adenocarcinomas of the pancreas in BOP-treated hamsters. In addition, iNOS expression was also observed in macrophages and islet cells in pancreatic tissue surrounding tumors. In order to assess the role of iNOS expression in carcinogenesis in the pancreas, the effects of ONO-1714 [(1*S*, 5*S*, 6*R*, 7*R*)-7-chloro-3-imino-5-methyl-2-azabicyclo[4.1.0]heptane], an iNOS inhibitor, on hamster pancreatic ductal carcinogenesis were investigated. Female Syrian golden hamsters were treated with BOP at 10 mg/kg body wt, four times for 1 week, and 1 week after the last carcinogen treatment, ONO-1714 was administered at doses of 100 and 200 p.p.m. in the diet for 15 weeks. The incidences and multiplicities of atypical hyperplasia and invasive adenocarcinoma and total adenocarcinomas (non-invasive and invasive adenocarcinomas) in the pancreas were significantly lowered by treatment with 200 p.p.m. ONO-1714. Treatment with 100 p.p.m. ONO-1714 also significantly decreased the multiplicities of invasive and total adenocarcinomas. Moreover, treatment with 200 p.p.m. ONO-1714 reduced the number of BOP-induced cholangiocellular tumors. These results suggest that iNOS plays roles in promoting pancreatic carcinogenesis in both early and late stages in hamsters.

Introduction

Pancreatic cancer is steadily increasing in incidence and has a very poor prognosis (1). For development of effective chemotherapeutic and chemopreventive agents, elucidation of causative factors and mechanisms underlying pancreatic carcinogenesis is very important. As with other cancers, chronic inflammation is considered to be one of the risk factors (2). Epidemiological studies have shown that in addition to the environmental factors like cigarette smoking and dietary habits, pancreatitis is very important (3). Causes of pancreatitis are known to include alcohol drinking, smoking, gallstones, hyperlipidemia and stress (4,5).

Abbreviations: BOP, *N*-nitrosobis(2-oxopropyl)amine; cDNA, complementary DNA; iNOS, inducible nitric oxide synthase; IL, interleukin; NO, nitric oxide; NOS, nitric oxide synthase.

Chronic inflammation is associated with release of many cytokines and activation of nuclear factor κB, resulting in the expression of nuclear factor κB-regulated, inflammatory-related genes, such as inducible nitric oxide synthase (iNOS) (6). The resultant overproduction of nitric oxide (NO) contributes to multistage carcinogenesis by inducing DNA mutations and tissue damage (6). Increased expression of iNOS in human pancreatic cancers has been described (7–9) and expression has been also reported in a rat pancreatitis model (10).

Suppressive effects of iNOS-selective inhibitors, (1*S*, 5*S*, 6*R*, 7*R*)-7-chloro-3-imino-5-methyl-2-azabicyclo[4.1.0] heptane (ONO-1714) and L-N^6-(1-iminoethyl)lysine tetrazole-amide (SC-51), on pancreatitis in rats have been reported (11,12). ONO-1714 is 10-fold more selective for human iNOS than for human endothelial nitric oxide synthase (NOS), very potent in inhibiting plasma NO elevation in lipopolysaccharide-treated mice with a 50% inhibition dose of 0.010 mg/Kg subcutaneously and less toxic with a maximum tolerated dose of 30 mg/kg intravenously in mice (13,14). In addition, ONO-1714 is effective even when orally administered and our previous studies have demonstrated suppressive effects of ONO-1714 on growth of tumors formed in nude mice after subcutaneous injection of the K-*ras* mutant-transfected cells (15), aberrant crypt focus formation and large tumor development in the colon of rats treated with azoxymethane (16) and on colon cancer development in Min mice treated with dextran sodium sulfate (17). However, to our knowledge, there have hitherto been no reports concerning effects of iNOS inhibitors on pancreatic cancer development.

The Syrian golden hamster provides a unique model animal for the development of ductal pancreatic cancer. With subcutaneous injections of *N*-nitrosobis(2-oxopropyl)amine (BOP) (18), lesions having close similarities to the major form of pancreatic cancer in humans are induced. Point mutations in codon 12 of the K-*ras* gene are frequently observed (19), and expression of the *fragile histidine triad* gene, a tumor suppression gene, is generally abnormal in pancreatic cancers of hamsters (20), as in human tumors (21,22). Upregulation of cyclooxygenase-2 has been also observed in both BOP-induced pancreatic neoplastic lesions in hamsters and in human lesions (23), although there has been no report of iNOS expression in hamster pancreatic cancer. Therefore in the present study, we examined expression of iNOS in hamster pancreatic ductal cancer and investigated suppressive effects of ONO-1714, an iNOS-selective inhibitor, on hamster pancreatic ductal carcinogenesis induced by BOP.

Materials and methods

Chemicals

(1*S*, 5*S*, 6*R*, 7*R*)-7-chloro-3-imino-5-methyl-2-azabicyclo[4.1.0] heptane (ONO-1714) was chemically synthesized at Ono Pharmaceutical Co. Ltd (Osaka, Japan). BOP was obtained from Nacalai Tesque (Kyoto, Japan).

Cell culture

A hamster pancreatic cancer cell line, HaP-T1 (24), was obtained from RIKEN Cell Bank (Saitama, Japan) and a hamster pancreatic β-cell cell line, HIT-T15, from Dainippon Pharmaceutical Co., Ltd (Osaka, Japan). Human pancreatic cancer cell lines, Capan-2, HPAF-II, HPAC, Hs-776T, MiaPaca-2 and Panc-1, were obtained from Summit Pharmaceutical International Co., LTD (Tokyo, Japan) and BxPC-3 from RIKEN Cell Bank. A human pancreatic normal ductal cell line, HPDE-6 (25), was kindly provided by Dr Ming-Sound Tsao (University Health Network, Toronto, Ontario, Canada). The cells were maintained in RPMI-1640 (Iwaki, Japan), supplemented with 5% fetal bovine serum (HyClone Laboratories, Logan, UT) and 100 units/ml penicillin–streptomycin (GIBCO/Invitrogen Corp., Carlsbad, CA) at 37°C in 5% CO_2. To induce iNOS expression, cells were treated with 10 ng/ml of mouse or human interleukin (IL)-1β (Sigma Chemical Co., St Louis, MO) for 6 h.

Animals

Five-week-old female Syrian golden hamsters weighing ~80 g were obtained from Japan SLC (Shizuoka, Japan) and acclimated to laboratory conditions for a week. They were housed two or three per plastic cage, with sterilized soft-wood chips as bedding, in an air-conditioned animal room, on a 12 h light–dark cycle. Powdered CE-2 (CLEA Japan, Shizuoka, Japan) was used as a standard basal diet. Body weights were measured on a weekly basis and food consumption twice a week. Food and water were made available *ad libitum*.

Reverse transcription–polymerase chain reaction analysis

Total RNA was extracted from culture cell samples using ISOGEN (Wako Pure Chemical Industries, Ltd, Osaka, Japan). After RNA purification, aliquots of total RNA (2 μg) were subjected to the reverse transcription reaction with oligo-dT or 9mer random primers in a final volume of 20 μl using an Omuniscript Reverse Transcription Kit (Qiagen GmbH, Heilden, Germany). Polymerase chain reaction amplification was performed in a final volume of 10 μl with aliquots of complementary DNA (cDNA) (25 ng) and iTaq DNA polymerase (Bio-Rad Laboratories, Hercules, CA) using a PTC-200 Peltier thermal cycler (MJ Research, Waltham, MA). The primers used were selected from the common sequences among hamster, mouse, rat and human cDNA sequences of β-actin (26) and the common sequences between hamster and human cDNA of iNOS (accession numbers, AY297461 and D26525)—5′-primer: ACGAGGCCCAGAGCAAGAGA, 3′-primer: TGGCTGGGGTGTTGAAGGTC (product size, 228 bp) for β-actin and 5′-primer: TTCCCCCAGCGGAGTGATGG, 3′-primer: GTACCAGCCATTGAAGGGGC (product size, 382 bp) for iNOS. The cycling conditions were as follows: 95°C for 3 min, 26 cycles (for β-actin) or 35 cycles (for iNOS) of 94°C for 15 s, 60°C for 25 s and 72°C for 30 s and a 10 min cycle at 72°C. Products were analyzed by 2% agarose gel electrophoresis with ethidium bromide staining.

Immunohistochemistry

Paraffin sections from formalin-fixed tissues of hamster normal pancreas and pancreatic tumors obtained in our previous study (26) were used for immunohistochemical analyses with the avidin–biotin complex immunoperoxidase technique as described previously (27). As the primary antibody, monoclonal mouse anti-iNOS IgG (BD Biosciences Pharmingen, San Diego, CA #610328) was applied at 50× dilution. As the secondary antibody, biotinylated anti-mouse IgG raised in a horse, affinity purified and absorbed with rat serum (Vector Laboratories, Burlingame, CA) was employed at 200× dilution. Staining was performed using avidin–biotin reagents (Vectastain ABC reagents; Vector Laboratories), 3,3′-diaminobenzidine and hydrogen peroxide. The sections were counterstained with hematoxylin. As a negative control, duplicate sections were immunostained without exposure to the primary antibody.

Study on the effects of ONO-1714, an iNOS inhibitor, on BOP-induced pancreatic carcinogenesis in hamsters

A total of 126 hamsters at 6 weeks of age were injected subcutaneously with BOP four times (on days 1, 3, 5 and 7) at a dose of 10 mg/kg body wt, whereas 18 hamsters received saline as vehicle controls. One week after the last BOP treatment, one-third of each group was given basal diet, diet containing 100 p.p.m. or 200 p.p.m. of ONO-1714 for 15 weeks. The doses were based on our previous study in mice (15,17) and rats (16) and a preliminary study in hamsters (data not shown). At the killing time point at 23 weeks of age, all surviving animals were anesthetized with diethyl ether, and blood samples were collected from the aorta. At autopsy, the pancreas, heart, lungs, kidneys, liver and bile duct were carefully examined macroscopically. The heart, lungs, kidneys, liver and bile duct were fixed in 10% phosphate-buffered formalin (pH 7.4). Each pancreas was carefully dissected from surrounding tissue and fixed after spreading on filter paper. All paraffin-embedded organs were sectioned and stained with hematoxylin and eosin for assessment of histopathological features, as described previously (26). The experimental protocol was in accordance with the guidelines for Animal Experiments in the National Cancer Center and was approved by the Institutional Ethics Review Committee for Animal Experimentation.

Statistical analysis

The significance of differences in the incidences of tumors was analyzed by the χ^2 test. Variation in other data was evaluated by the Student's *t*-test. A *P* value of <0.05 was regarded as significant.

Results

iNOS expression in human and hamster pancreatic cancer cell lines

Expression of iNOS messenger RNA in human and hamster pancreatic cancer cell lines was examined by reverse transcription–polymerase chain reaction. As shown in Figure 1, iNOS was constitutively

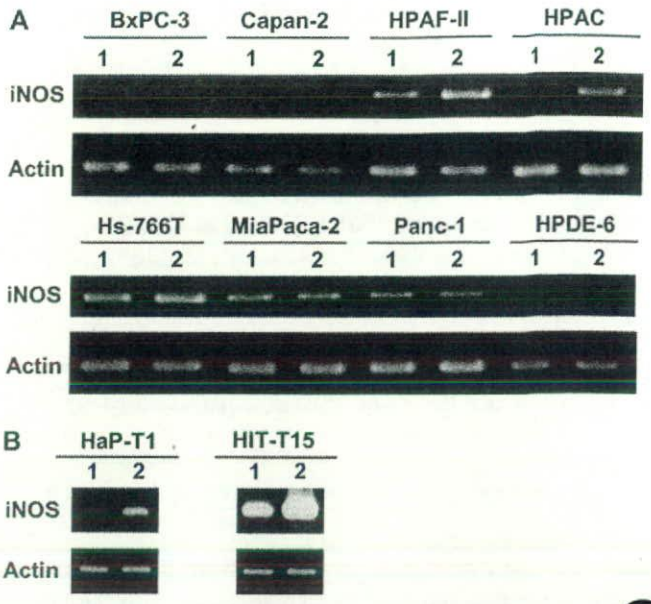

Fig. 1. Reverse transcription–polymerase chain reaction analysis of iNOS expression in human (**A**) and hamster (**B**) pancreatic cell lines. Pancreatic cancer cell lines (BxPC-3, Capan-2, HPAF-II, HPAC, Hs-766T, MiaPaca-2, Panc-1 and HaP-T1), a normal pancreatic ductal epithelial cell line (HPDE-6) and an islet β-cell line (HIT-T15) were incubated in basal medium (lane 1) or treated with 10 ng/ml IL-1β (lane 2) for 6 h. Total RNA from each sample was extracted and cDNA was synthesized by reverse transcription. Then, cDNA fragments of iNOS and β-actin were amplified by polymerase chain reaction, and the polymerase chain reaction products were electrophoresed on a 2% agarose gel.

expressed in five of seven human pancreatic cancer cell lines, BxPC-3, HPAF-II, Hs-766T, MiaPaca-2 and Panc-1. On treatment with IL-1β, expression of iNOS in the other two cancer cell lines, Capan-2 and HPAC, and a human pancreatic normal ductal cell line, HPDE-6, was induced, and the expression in HPAF-II and Hs-766T was enhanced. Expression of iNOS was also constitutively observed in a hamster pancreatic cancer cell line, HaP-T1, and a hamster β-cell cell line, HIT-T15, and in both cases was markedly enhanced by treatment with IL-1β.

iNOS expression in hamster pancreatic ductal adenocarcinoma induced by BOP

Expression of iNOS protein in hamster pancreatic ductal cancers was examined by immunohistochemical staining. In normal pancreatic tissue, expression of iNOS protein was barely detectable in non-treated normal pancreatic tissue (Figure 2A) and non-tumorous parts of BOP-treated pancreatic tissue (Figure 2B). In contrast, positive staining for iNOS was clearly observed in macrophages and islet cells in areas of inflammation, atypical hyperplasia in ducts (Figure 2C) and in the carcinoma epithelial cells (Figure 2D). All 12 pancreatic carcinomas examined were positive for iNOS staining: six demonstrated strong, four moderate and two weak staining in the cytoplasm of epithelial cancer cells.

Effects of ONO-1714 on pancreatic tumor development in BOP-treated hamsters

To examine the role of iNOS on pancreatic carcinogenesis, hamsters were treated with a pancreatic carcinogen, BOP, then were fed a diet containing the iNOS inhibitor, ONO-1714, at doses of 100 or 200 p.p.m. for 15 weeks. The final body weights (g) and average food intake of hamsters are shown in Table I. The body weights and average food intake in the BOP + basal diet group were lower than those in the saline + basal diet group ($P < 0.05$), and the average body weight in the saline + 200 p.p.m. ONO-1714 group was 13% lower

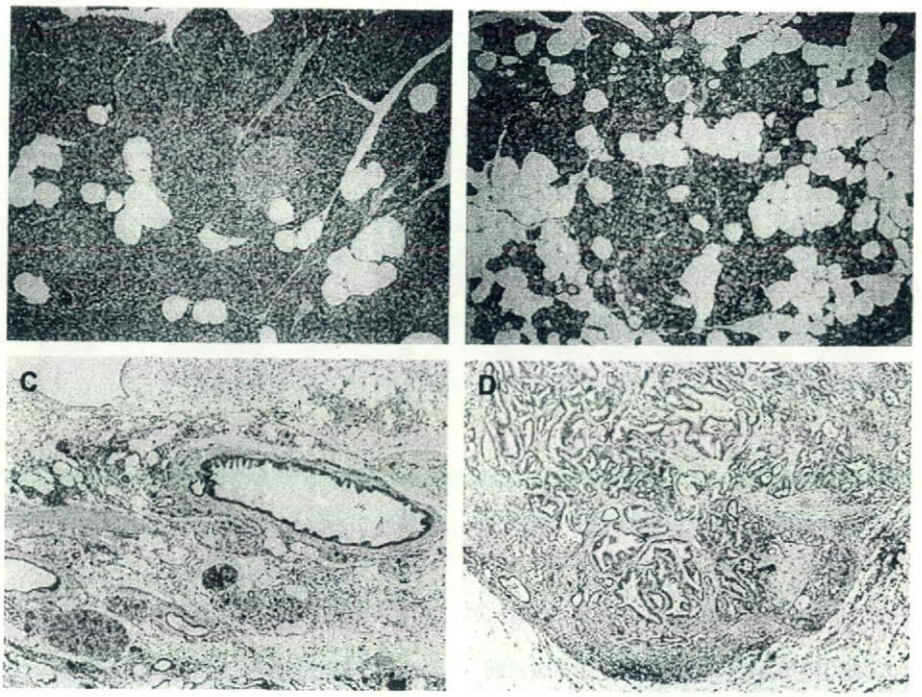

Fig. 2. Immunohistochemical staining for iNOS. No iNOS immunoreactivity is apparent in normal pancreas of non-treated (**A**) and BOP-treated (**B**) hamsters. Immunoreactive iNOS is observed in macrophages and islet cells in inflammation, atypical hyperplasia in ducts (**C**) and carcinoma epithelial cells (**D**) in BOP-treated hamsters. (**A–D**) ×100.

than in the saline + basal diet group ($P < 0.01$). However, in the BOP-treated groups, no significant differences were observed after treatment with ONO-1714.

Pancreatic lesions were histopathologically diagnosed as atypical hyperplasia, non-invasive adenocarcinomas and invasive adenocarcinomas. Incidence and multiplicity data are summarized in Table II. The incidence of atypical hyperplasia and adenocarcinomas induced by BOP was lower in the group treated with 200 p.p.m. ONO-1714 than in the control group (21 versus 52% at $P < 0.005$ and 45 versus 69% at $P < 0.05$, respectively). Remarkably, the incidence of invasive adenocarcinomas was significantly lower in the 200 p.p.m. ONO-1714 group than in the control group (12 versus 45% at $P < 0.001$). Multiplicities of total adenocarcinomas were significantly decreased by treatment with 100 p.p.m. (0.76 ± 0.82, $P < 0.05$) and 200 p.p.m. ONO-1714 (0.60 ± 0.77, $P < 0.01$) compared with the control value (1.19 ± 1.10). It was notable that the multiplicities of invasive adenocarcinomas in the 100 p.p.m. and 200 p.p.m. ONO-1714 groups were only one-half (0.36 ± 0.62, $P < 0.05$) and one-fifth (0.14 ± 0.42, $P < 0.01$) of the control value (0.74 ± 1.01), respectively. On the other hand, the multiplicities of non-invasive adenocarcinomas did not significantly differ among the three groups. Figure 3 shows the size distribution of pancreatic adenocarcinomas. The numbers of carcinomas <3, 3–5 and ≥5 mm in diameter in the BOP + 100 p.p.m. ONO-1714 group were 55, 56 and 86% of the BOP + basal diet values, respectively, suggesting that treatment with 100 p.p.m. ONO-1714 tended to suppress the development of carcinomas <5 mm in diameter, but not the larger lesions. On the other hand, those in the BOP + 200 p.p.m. ONO-1714 group were 75, 38 and 29% of the control group, respectively, indicating that treatment with 200 p.p.m. ONO-1714 tended to suppress the development of carcinoma >3 mm in diameter and significantly reduced the development of carcinoma >5 mm in diameter ($P < 0.05$).

In addition to pancreatic ductal tumors, tumors of the bile duct, liver, lungs and kidneys have been reported to be induced by BOP in hamsters (18). In the present study, hepatocellular and cholangiocellular tumors were observed in the BOP-treated group at incidences of 12 and 50%, respectively (Table III). The cholangiocellular tumors developed in both intra- and extrahepatic bile ducts. The incidences of hepatocellular and cholangiocellular tumors were not significantly changed by ONO-1714 administration, but the multiplicity of cholangiocellular tumors was significantly decreased by 200 p.p.m. ONO-1714 treatment compared with the controls (0.38 ± 0.66 versus 1.14 ± 1.57 at $P < 0.005$) (Table III).

In contrast, the incidences and multiplicities of lung tumors were statistically increased by 100 p.p.m. ONO-1714 [33/42 (79%) at $P < 0.05$ and 1.60 ± 1.29 at $P < 0.05$, respectively] and slightly but not significantly by 200 p.p.m. ONO-1714 [26/42 (62%) and 1.26 ± 1.33, respectively] compared with the control group [21/42 (50%) and 0.98 ± 1.42, respectively]. A renal mesenchymal tumor and a hemangioma were observed in the BOP + basal diet group, an angiosarcoma in the BOP + 100 p.p.m. ONO-1714 group and a nephroblastoma in the BOP + 200 p.p.m. ONO-1714 group, but their incidences were not significant. Tumors in the pancreatic duct, bile duct, liver, lungs and kidneys were not observed in the saline vehicle ($n = 15$) or 100 p.p.m. and 200 p.p.m. ONO-1714 group hamsters without the BOP treatment ($n = 15$, each).

Table I. Final body weights of the hamsters and average food intake

Treatment	No. of animals	Final body weight (g)	Food intake[a] (g/hamster/day)
BOP + basal diet	42	199 ± 21[b,c]	10.8 ± 0.4[c]
BOP + 100 p.p.m. ONO-1714	42	200 ± 17	11.0 ± 0.6
BOP + 200 p.p.m. ONO-1714	42	193 ± 19	10.5 ± 0.5
Saline + basal diet	6	219 ± 18	11.7 ± 1.0
Saline + 100 p.p.m. ONO-1714	6	194 ± 22	10.8 ± 0.1
Saline + 200 p.p.m. ONO-1714	6	190 ± 13[d]	10.1 ± 0.1

[a]Total food intake of each animal cage for 15 weeks was divided by animal number in each cage and the total period (days).
[b]Data are mean ± SD.
[c]Significantly different from the saline + basal diet group at $P < 0.05$.
[d]Significantly different from the saline + basal diet group at $P < 0.01$.

Table II. Effects of ONO–1714 treatment on the incidences and multiplicities of pancreatic lesions induced by BOP[a]

Dose of ONO-1714 in diet	Effective no. of animals	No. of animals with lesions (%)				No. of lesions in the pancreas			
		Atypical hyperplasia	Ductal adenocarcinoma			Atypical hyperplasia	Ductal adenocarcinoma		
			Non-invasive	Invasive	Total[b]		Non-invasive	Invasive	Total[b]
0 p.p.m.	42	22 (52)[c]	15 (36)	19 (45)	29 (69)	0.57 ± 0.59[d]	0.45 ± 0.71	0.74 ± 1.01	1.19 ± 1.10
100 p.p.m.	42	24 (57)	13 (31)	12 (29)	24 (57)	0.69 ± 0.68	0.40 ± 0.70	0.36 ± 0.62*	0.76 ± 0.82*
200 p.p.m.	42	9 (21)**	15 (36)	5 (12)***	19 (45)*	0.29 ± 0.64	0.45 ± 0.71	0.14 ± 0.42***	0.60 ± 0.77**

[a]Hamsters were fed a basal diet or a diet containing ONO-1714, an iNOS inhibitor, for 15 weeks.
[b]The total represents animals with non-invasive and/or invasive carcinomas.
[c]Percentages in parentheses.
[d]Data are mean ± SD values.
Significantly different from the control group at $^{*}P < 0.05$, $^{**}P < 0.005$ and $^{***}P < 0.001$.

Discussion

The present study demonstrated that iNOS is expressed in pancreatic cancer cells and that the iNOS inhibitor, ONO-1714, can effectively suppress the development of atypical hyperplasia and cancer, especially invasive cancers, in the hamster pancreas after treatment with BOP. The results indicated that iNOS plays important roles in the development of preneoplastic lesions at an early stage of pancreatic carcinogenesis and also in cancer invasion and expansion in later stages.

In our previous study of colon carcinogenesis, ONO-1714 suppressed the development of rat colon tumors >3 mm in diameter (16), in line with the present findings. It has been reported that angiogenesis is necessary to supply oxygen and nutrients to solid tumors >1–2 mm^3 in size (28). NO enhances vascular permeability, partly through activation of matrix metalloproteinases (29), suggesting that suppression of the development of large tumors in ONO-1714-treated groups may be associated with inhibition of angiogenesis by the iNOS inhibitor.

Expression of iNOS has been detected in more than half of human pancreatic cancers (7–9). Here, iNOS expression was observed in most of the hamster pancreatic cancers and atypical hyperplasia. In the BOP-induced pancreatic ductal carcinogenesis model in hamsters, G to A transitions at the second base of the codon 12 of the K-*ras* gene have been shown to be quite frequent in pancreatic cancers and even in preneoplastic lesions at lower frequency (30). Our previous study revealed that iNOS expression can be markedly elevated by transfection of K-*ras* mutant cDNA into IEC-6 rat intestinal epithelial cells in the presence of IL-1β or lipopolysaccharide through the activation of promoters on nuclear factor κB, C/EBP and CRE-like sites and that growth of tumors formed in nude mice by subcutaneous injection of the K-*ras* mutant-transfected cells can be suppressed by feeding diets containing NOS inhibitors (15). It is feasible that iNOS expression in pancreatic cancers could also be associated with K-ras activation. Indeed, human pancreatic cancers frequently harbor K-*ras* mutations (21,31–33) and other cancers with frequent K-*ras* mutations, such as colon (32,33), lung (33) and intrahepatic bile duct carcinomas (34), also show increased iNOS expression (35–37). Thus, NO produced by iNOS may be generally involved in tumor development by activated K-ras, and iNOS-selective inhibitors should be considered as possible candidates for the prevention of all cancers featuring K-ras activation.

K-*ras* mutations are observed from early stages of carcinogenesis in the pancreas, colon, lungs (30,33) and intrahepatic bile ducts (38). Our previous studies in the azoxymethane-induced rat colon carcinogenesis model showed frequent K-*ras*-activating mutations in hyperplastic aberrant crypt foci (39) and suppression of aberrant crypt focus development by the iNOS inhibitor ONO-1714 (16). The present study also showed iNOS expression in precancerous lesions and suppression of the development of atypical hyperplasia in the pancreas of hamsters by an iNOS inhibitor. It can thus be concluded that

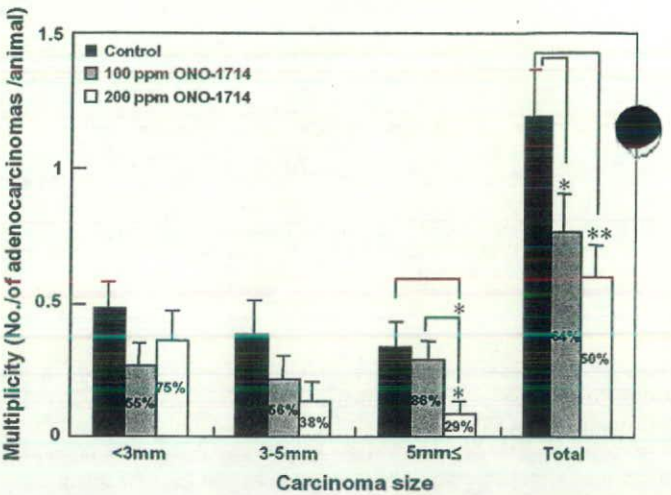

Fig. 3. Effects of ONO-1714 treatment on the sizes of pancreatic cancers. The numbers of each size of pancreatic cancers per hamster are given for the BOP + 0 p.p.m. ONO-1714 (black bars), BOP + 100 p.p.m. ONO-1714 (gray bars) and BOP + 200 p.p.m. ONO-1714 (white bars) groups (mean ± standard error values). * and ** Significantly different from the respective controls at $P < 0.05$ and $P < 0.01$, respectively. The percentage of the BOP + basal diet control value is shown in each column.

K-ras-enhanced iNOS expression may contribute to the development of early precancerous lesions.

It has been reported that IL-1β induces iNOS expression in pancreatic β-cells (40), and overproduction of NO causes dysfunction and destruction of β-cells (41). In the present study, iNOS expression in pancreatic islets surrounded by cancer-associated inflammation was observed. Epidemiological studies have reported that diabetes mellitus is also a risk factor for pancreatic cancer (3). Therefore, increased expression of iNOS in pancreatic islets may also be involved in pancreatic carcinogenesis and iNOS inhibitors might also be protective against autoimmune diabetes.

In the present study, the iNOS inhibitor ONO-1714 significantly suppressed the development of pancreatic cancer and cholangiocellular tumors, but not of lung tumors. Pancreatic ductal adenocarcinomas and cholangiocellular tumors in BOP-treated hamsters have certain genetic characteristics in common; for example, K-*ras* mutations and aberrant transcription of the *fragile histidine triad* gene were observed in both (19,20,38,42). Expression of iNOS was also observed in cholangiocellular tumors obtained in the present study (data not shown). It could be speculated that the influence of the iNOS inhibitor might be similar for the two types of carcinoma, one arising from ducts in the pancreas and the other from bile ducts. In contrast, treatment with 100 p.p.m. but not 200 p.p.m. ONO-1714 rather enhanced development of

Table III. Effects of ONO–1714 treatment on the incidences and multiplicities of liver and bile duct tumors induced by BOP[a]

Dose of ONO-1714 in diet	Effective no. of animals	No. of animals with tumors (%)				No. of tumors in the liver			
		Hepatocellular adenoma	Cholangiocellular tumors			Hepatocellular adenoma	Cholangiocellular tumors		
			Adenoma	Adenocarcinoma	Total[b]		Adenoma	Adenocarcinoma	Total[b]
0 p.p.m.	42	5 (12)[c]	19 (45)	4 (10)	21 (50)	0.12 ± 0.33[d]	1.02 ± 1.52	0.12 ± 0.40	1.14 ± 1.57
100 p.p.m.	42	2 (5)	23 (55)	2 (5)	24 (57)	0.05 ± 0.22	0.76 ± 0.88	0.07 ± 0.34	0.83 ± 0.91
200 p.p.m.	42	3 (7)	12 (29)	3 (7)	13 (31)	0.07 ± 0.26	0.31 ± 0.52*	0.07 ± 0.26	0.38 ± 0.66**

[a]Hamsters were fed a basal diet or a diet containing ONO-1714, an iNOS inhibitor, for 15 weeks.
[b]The total represents animals with non-invasive and/or invasive carcinomas.
[c]Percentages in parentheses.
[d]Data are mean ± SD values.
Significantly different from the control group at $^{*}P < 0.01$ and $^{**}P < 0.005$.

lung tumors. It has been reported that several NOS inhibitors are chemopreventive in the rat tracheal epithelial cell transformation system (43). Reduction in lung tumor development in iNOS(−/−) mice has also been reported (44), suggesting that iNOS expression is associated with lung tumorigenesis. However, endothelial NOS and neuronal NOS are also expressed in lung tumors and high total expression levels of the three NOS types have been suggested to be a favorable prognostic sign (45). Thus, it appears that data on roles of NO in lung tumorigenesis are contradictory and the promotive effect of iNOS is not yet conclusive. Interestingly, other chemopreventive agents reported, such as 4-phenylbutyl isothiocyanate (46), phenethyl isothiocyanate (47) and a cyclooxygenase inhibitor, nimesulide (48) suppressed pancreatic cancers and lung tumors, but enhanced (46) or did not affect (47,48) liver tumorigenesis in BOP-treated hamsters. Thus, it can be presumed that the inhibitory mechanisms of these agents on pancreatic cancer may be different from that of ONO-1714. Our previous study on the prevention of hamster pancreatic carcinogenesis by a peroxisome proliferator-activated receptor γ ligand, pioglitazone, also showed significant suppression of the development of pancreatic ductal adenocarcinomas and cholangiocellular tumors, but not of lung adenomas (26). It is known that peroxisome proliferator-activated receptor γ activation inhibits cytokine-mediated iNOS expression (49,50), indicating that inhibitory mechanisms of ONO-1714 and pioglitazone on hamster pancreatic carcinogenesis could be shared, at least in part.

In conclusion, the present study demonstrated probable involvement of iNOS expression in hamster pancreatic ductal carcinogenesis, and suppression of development of pancreatic atypical hyperplasia and invasive adenocarcinomas by treatment with an iNOS inhibitor. Thus, it is proposed that iNOS inhibitors might be promising chemopreventive agents against pancreatic cancer.

Funding

Grants-in-Aid for Cancer Research (18-5,19-2); Third-Term Comprehensive 10-Year Strategy for Cancer Control (H19-013) from the Ministry of Health, Labour and Welfare of Japan.

Acknowledgements

We thank Ms Ayami Etoh and Mr Naoaki Uchiya for expert technical assistance. T.Kitahashi was the awardee of Research Resident Fellowship from the Foundation for Promotion of Cancer Research (Japan) for the Third-Term Comprehensive 10 Year Strategy for Cancer Control during the performance of this study.

Conflict of Interest Statement: None declared.

References

1. Parkin,D.M. *et al.* (2001) Estimating the world cancer burden: Globocan 2000. *Int. J. Cancer*, **94**, 153–156.
2. Farrow,B. *et al.* (2002) Inflammation and the development of pancreatic cancer. *Surg. Oncol.*, **10**, 153–169.
3. Michaud,D.S. (2004) Epidemiology of pancreatic cancer. *Minerva. Chir.*, **59**, 99–111.
4. Otsuki,M. *et al.* (2007) 4. Chronic pancreatitis and pancreatic cancer, lifestyle-related diseases. *Intern. Med.*, **46**, 109–113.
5. Kemppainen,E. *et al.* (2007) Non-alcoholic etiologies of acute pancreatitis—exclusion of other etiologic factors besides alcohol and gallstones. *Pancreatology*, **7**, 142–146.
6. Hussain,S.P. *et al.* (2007) Inflammation and cancer: an ancient link with novel potentials. *Int. J. Cancer*, **121**, 2373–2380.
7. Vickers,S.M. *et al.* (1999) Association of increased immunostaining for inducible nitric oxide synthase and nitrotyrosine with fibroblast growth factor transformation in pancreatic cancer. *Arch. Surg.*, **134**, 245-251.
8. Kong,G. *et al.* (2001) Inducible nitric oxide synthase (iNOS) immunoreactivity and its relationship to cell proliferation, apoptosis, angiogenesis, clinicopathologic characteristics, and patient survival in pancreatic cancer. *Int. J. Pancreatol.*, **29**, 133–140.
9. Kong,G. *et al.* (2002) Role of cyclooxygenase-2 and inducible nitric oxide synthase in pancreatic cancer. *J. Gastroenterol. Hepatol.*, **17**, 914–921.
10. Al-Mufti,R.A. *et al.* (1998) Increased nitric oxide activity in a rat model of acute pancreatitis. *Gut*, **43**, 564–570.
11. Mikawa,K. *et al.* (2001) ONO-1714, a new inducible nitric oxide synthase inhibitor, attenuates diaphragmatic dysfunction associated with cerulein-induced pancreatitis in rats. *Crit. Care Med.*, **29**, 1215–1221.
12. Sandstrom,P. *et al.* (2005) Highly selective inhibition of inducible nitric oxide synthase ameliorates experimental acute pancreatitis. *Pancreas*, **30**, e10–e15.
13. Naka,M. *et al.* (2000) A potent inhibitor of inducible nitric oxide synthase, ONO-1714, a cyclic amidine derivative. *Biochem. Biophys. Res. Commun.*, **270**, 663–667.
14. Hayashi,Y. *et al.* (2005) Comparison of effects of nitric oxide synthase (NOS) inhibitors on plasma nitrite/nitrate levels and tissue NOS activity in septic organs. *Microbiol. Immunol.*, **49**, 139–147.
15. Takahashi,M. *et al.* (2003) Transfection of K-*ras*^{Asp12} cDNA markedly elevates IL-1β and lipopolysaccharide-mediated inducible nitric oxide synthase expression in rat intestinal epithelial cells. *Oncogene*, **22**, 7667–7676.
16. Takahashi,M. *et al.* (2006) Suppressive effect of an inducible nitric oxide inhibitor, ONO-1714, on AOM-induced rat colon carcinogenesis. *Nitric Oxide*, **14**, 130–136.
17. Kohno,H. *et al.* (2007) A specific nitric oxide synthase inhibitor, ONO-1714 attenuates inflammation-related large bowel carcinogenesis in male Apc(Min/+) mice. *Int. J. Cancer*, **121**, 506–513.
18. Pour,P. *et al.* (1977) A potent pancreatic carcinogen in Syrian hamsters: *N*-nitrosobis(2-oxopropyl)amine. *J. Natl Cancer Inst.*, **58**, 1449–1453.
19. Fujii,H. *et al.* (1991) Pancreatic ductal adenocarcinomas induced in Syrian hamsters by *N*-nitrosobis(2-oxopropyl)amine contain a c-Ki-ras oncogene with a point-mutated codon 12. *Mol. Carcinog.*, **3**, 296–301.
20. Tsujiuchi,T. *et al.* (2003) Alterations in the *Fhit* gene in pancreatic duct adenocarcinomas induced by *N*-nitrosobis(2-oxopropyl)amine in hamsters. *Mol. Carcinog.*, **36**, 60–66.
21. Grunewald,K. *et al.* (1989) High frequency of *Ki-ras* codon 12 mutations in pancreatic adenocarcinomas. *Int. J. Cancer*, **43**, 1037–1041.
22. Sorio,C. *et al.* (1999) The *FHIT* gene is expressed in pancreatic ductular cells and is altered in pancreatic cancers. *Cancer Res.*, **59**, 1308–1314.
23. Crowell,P.L. *et al.* (2006) Cyclooxygenase-2 expression in hamster and human pancreatic neoplasia. *Neoplasia*, **8**, 437–445.

24. Saito,S. *et al.* (1988) Establishment and characterization of a cultured cell line derived from nitrosamine-induced pancreatic ductal adenocarcinoma in Syrian golden hamsters. *Gastroenterol. Jpn.*, **23**, 183–194.
25. Furukawa,T. *et al.* (1996) Long-term culture and immortalization of epithelial cells from normal adult human pancreatic ducts transfected by the E6E7 gene of human papilloma virus 16. *Am. J. Pathol.*, **148**, 1763–1770.
26. Takeuchi,Y. *et al.* (2007) Suppression of *N*-nitrosobis(2-oxopropyl)amine-induced pancreatic carcinogenesis in hamsters by pioglitazone, a ligand of peroxisome proliferator-activated receptor gamma. *Carcinogenesis*, **28**, 1692–1696.
27. Takahashi,M. *et al.* (1997) Increased expression of inducible and endothelial constitutive nitric oxide synthases in rat colon tumors induced by azoxymethane. *Cancer Res.*, **57**, 1233–1237.
28. Folkman,J. (1990) What is the evidence that tumors are angiogenesis dependent? *J. Natl Cancer Inst.*, **82**, 4–6.
29. Wu,J. *et al.* (2001) Enhanced vascular permeability in solid tumor involving peroxynitrite and matrix metalloproteinases. *Jpn. J. Cancer Res*, **92**, 439–451.
30. Cerny,W.L. *et al.* (1992) K-*ras* mutation is an early event in pancreatic duct carcinogenesis in the Syrian golden hamster. *Cancer Res.*, **52**, 4507–4513.
31. Mu,D.Q. *et al.* (2004) Values of mutations of K-*ras* oncogene at codon 12 in detection of pancreatic cancer: 15-year experience. *World J. Gastroenterol.*, **10**, 471–475.
32. Burmer,G.C. *et al.* (1991) Frequency and spectrum of c-Ki-*ras* mutations in human sporadic colon carcinoma, carcinomas arising in ulcerative colitis, and pancreatic adenocarcinoma. *Environ. Health Perspect.*, **93**, 27–31.
33. Minamoto,T. *et al.* (2000) K-*ras* mutation: early detection in molecular diagnosis and risk assessment of colorectal, pancreas, and lung cancers—a review. *Cancer Detect. Prev.*, **24**, 1–12.
34. Acalovschi,M. (2004) Cholangiocarcinoma: risk factors, diagnosis and management. *Rom. J. Intern. Med.*, **42**, 41–58.
35. Ambs,S. *et al.* (1998) Frequent nitric oxide synthase-2 expression in human colon adenomas: implication for tumor angiogenesis and colon cancer progression. *Cancer Res.*, **58**, 334–341.
36. Liu,C.-Y. *et al.* (1998) Increased level of exhaled nitric oxide and up-regulation of inducible nitric oxide synthase in patients with primary lung cancer. *Br. J. Cancer*, **78**, 534–541.
37. Pinlaor,S. *et al.* (2005) Nitrative and oxidative DNA damage in intrahepatic cholangiocarcinoma patients in relation to tumor invasion. *World J. Gastroenterol.*, **11**, 4644–4649.
38. Yamanaka,S. *et al.* (1997) K-ras gene mutations in intrahepatic bile duct of Syrian golden hamsters. *J. Surg. Oncol.*, **66**, 97–103.
39. Takahashi,M. *et al.* (2000) Altered expression of β-catenin, inducible nitric oxide synthase and cyclooxygenase-2 in azoxymethane-induced rat colon carcinogenesis. *Carcinogenesis*, **21**, 1319–1327.
40. Kwon,G. *et al.* (1995) Interleukin-1 beta-induced nitric oxide synthase expression by rat pancreatic beta-cells: evidence for the involvement of nuclear factor kappa B in the signaling mechanism. *Endocrinology*, **136**, 4790–4795.
41. McDaniel,M.L. *et al.* (1996) Cytokines and nitric oxide in islet inflammation and diabetes. *Proc. Soc. Exp. Biol. Med.*, **211**, 24–32.
42. Kitahashi,T. *et al.* (2004) Aberrant transcription of *FHIT* gene in intrahepatic cholangiocellular carcinomas induced by *N*-nitrosobis(2-oxopropyl)amine in hamsters. *Exp. Toxicol. Pathol.*, **56**, 153–157.
43. Sharma,S. *et al.* (2002) Differential activity of NO synthase inhibitors as chemopreventive agents in a primary rat tracheal epithelial cell transformation system. *Neoplasia*, **4**, 332–336.
44. Kisley,L.R. *et al.* (2002) Genetic ablation of inducible nitric oxide synthase decreases mouse lung tumorigenesis. *Cancer Res.*, **62**, 6850–6856.
45. Puhakka,A. *et al.* (2003) High expression of nitric oxide synthases is a favorable prognostic sign in non-small cell lung carcinoma. *APMIS*, **111**, 1137–1146.
46. Son,H.-Y. *et al.* (2000) Modifying effects of 4-phenylbutyl isothiocyanate on *N*-nitrosobis(2-oxopropyl)amine-induced tumorigenesis in hamsters. *Cancer Lett.*, **160**, 141–147.
47. Nishikawa,A. *et al.* (1996) Chemopreventive effects of phenethyl isothiocyanate on lung and pancreatic tumorigenesis in *N*-nitrosobis(2-oxopropyl)amine-treated hamsters. *Carcinogenesis*, **17**, 1381–1384.
48. Furukawa,F. *et al.* (2003) A cyclooxygenase-2 inhibitor, nimesulide, inhibits postinitiation phase of *N*-nitrosobis(2-oxopropyl)amine-induced pancreatic carcinogenesis in hamsters. *Int. J. Cancer*, **104**, 269–273.
49. Beauregard,C. *et al.* (2003) Peroxisome proliferator-activated receptor agonists inhibit interleukin-1beta-mediated nitric oxide production in cultured lacrimal gland acinar cells. *J. Ocul. Pharmacol. Ther.*, **19**, 579–587.
50. Crosby,M.B. *et al.* (2005) A novel PPAR response element in the murine iNOS promoter. *Mol. Immunol.*, **42**, 1303–1310.

Received April 9, 2008; revised June 5, 2008; accepted June 9, 2008

Relationships between intestinal polyp formation and fatty acid levels in plasma, erythrocytes, and intestinal polyps in Min mice

Kiyonori Kuriki,[1,2,6] Michihiro Mutoh,[3] Kazuo Tajima,[1,4] Keiji Wakabayashi[3] and Masae Tatematsu[2,5]

[1]Division of Epidemiology and Prevention, [2]Division of Oncological Pathology, Aichi Cancer Center Research Institute, 1-1 Kanokoden, Chikusa-ku, Nagoya 464-8681; [3]Cancer Prevention Basic Research Project, National Cancer Research Institute, 5-1-1 Tsukiji, Chuo-ku, Tokyo 104-0045; [4]Department of Epidemiology, [5]Division of Cancer Genetics, Nagoya University Graduate School of Medicine, 65 Tsurumai-Cho, Showa-ku, Nagoya, 466-8550, Japan

(Received July 1, 2008/Revised August 12, 2008/Accepted August 19, 2008/Online publication November 25, 2008)

We have reported that a hyperlipidemic state is characteristic of *Apc*-deficient Min mice with multiple intestinal polyps. In our earlier case-control study, colorectal cancer risk showed positive relationships with erythrocyte membrane compositions of palmitic and oleic acids, but negative links with linoleic and arachidonic acids. To examine the roles of fatty acids in intestinal polyp formation, levels in plasma, erythrocytes, and intestinal polyps in Min mice were compared with those in wild-type mice. A diet free of eicosapentaenoic and docosahexaenoic acids with antineoplastic effects was fed to all mice from 6 to 15 weeks of age. Fatty acid levels were measured using accelerated solvent extraction and gas–liquid chromatography. Min mice with a hyperlipidemic state and multiple intestinal polyps had elevated values for palmitic and oleic acids in plasma and erythrocytes (at least $P < 0.05$), and higher plasma level of linoleic acid ($P < 0.05$). Arachidonic acid was 24.5% lower in erythrocytes ($P < 0.0005$), but did not differ in plasma. In Min mice, moreover, oleic and arachidonic acids were 1.78 and 1.43 times higher, respectively, in intestinal polyps than in paired normal mucosa ($P < 0.05$ and $P < 0.01$, respectively), but linoleic acid was 31.9% lower ($P < 0.001$). The present study suggests that palmitic, oleic, and arachidonic acids play key roles in intestinal polyp formation, and demonstrates reduced erythrocyte arachidonic acid values of Min mice, in line with our previous findings for patients with sporadic colorectal cancers. (*Cancer Sci* 2008; 99: 2410–2416)

A high-fat diet, especially animal fat or SFA, is suggested to increase the likelihood of colorectal cancer,[1] but the cited risk impacts for the amount and various types of fatty acid intakes have varied with study. There is some evidence that the risk of sporadic colorectal adenomasis is positively linked to the prevalence of hyperlipidemiam,[2–4] and serum levels of triglycerides are slightly higher in FAP patients with cancer than in those without cancer.[5] *APC* mutations found in FAP patients are linked to the development of multiple intestinal polyps, also being frequently observed in patients with sporadic colorectal cancers. Compared with the corresponding wild-type mice, we also have demonstrated that serum levels of triglycerides are approximately 10 times higher in *Apc* gene-deficient Min ($C57BL/6\text{-}APC^{Min/+}$) and APC^{1309} ($C57BL/6J^{APC/APC\ 1309}$) mice, with the increases being suppressed by PPAR ligands and a specific reagent (NO-1886) that increases LPL, an enzyme that catalyzes the hydrolysis of triglycerides.[6–8] Therefore, a hyperlipidemic state has been suggested to be related to polyp formation in the intestinal tract.

Using biomarkers for dietary intake of fish rich in EPA and DHA for mid- to long-term intakes, we have recently shown the sporadic risk of colorectal cancer to be negatively linked to erythrocyte membrane values of EPA and DHA.[9] We simultaneously observed that increased risk was related to palmitic and oleic acid levels and that reduced risk was associated with high linoleic acid and AA values. The following issues, however, were not clarified: (1) whether there are relationships between tumor development and values for palmitic and oleic acids; and (2) why there was a discrepancy in the generally accepted roles of the AA cascade, that is, the generation of prostaglandin E_2, which is linked to inflammation, tumorigenesis, anigiogenesis, cell proliferation, and inhibition of apoptosis.

To clarify the relationships between polyp formation and fatty acid levels in the intestinal tract, we examined the influence of fatty acids on intestinal polyp formation in Min mice fed a diet free of EPA and DHA. The present animal study was designed with the following features. First, we used *Apc*-deficient Min mice, which have been investigated extensively for mechanisms of intestinal tumor development. Second, carcinogenic chemicals such as azoxymethane were not used because their metabolism in the liver might be affected by fatty acid metabolism. Third, a diet free of EPA and DHA was fed to all mice because antineoplasia effects of these two fatty acids have been demonstrated in many laboratory studies. In the present study, a typical diet used in research was fed to all mice. Fourth, fatty acid levels in small amounts of biomaterials were measured by a newly developed analytical method, using an automatic solvent extractor and gas–liquid chromatography.[10] Fifth, we measured fatty acid levels in a series of biomaterials: plasma, erythrocyte membranes, and intestinal polyps (or normal mucosa).

Materials and Methods

Animals and chemicals. Male $C57BL/6\text{-}APC^{Min/+}$ mice (Min mice) were purchased from the Jackson Laboratory (Bar Harbor, ME, US) at 6 weeks of age and genotyped by a method reported elsewhere.[11] We used male animals for experimental convenience because there are no reported significant differences in serum lipid levels or the numbers of intestinal polyps between male and female mice.[6–8,12] Ten heterozygotes of the Min strain and five wild-type (C57BL/6J) mice were acclimated to laboratory conditions for 9 weeks, and housed per plastic cage with sterilized softwood chips as bedding in a barrier-sustained animal room airconditioned at 24 ± 2°C and 55% humidity on a 12:12 h light : dark cycle.

Animal experiments. An AIN-76A diet free of EPA and DHA was obtained from Clea Japan (Tokyo, Japan). The diet and

[6]To whom correspondence should be addressed. E-mail: kkuriki@aichi-cc.jp

Abbreviations: AA, arachidonic acid; APC, adenomatous polyposis coli; DHA, docosahexaenoic acid; EPA, eicosapentaenoic acid; FAP, familial adenomatous polyposis; LPL, lipoprotein lipase; MUFA, monounsaturated fatty acid; PPAR, peroxisome proliferator activated receptor; PUFA, polyunsaturated fatty acid; SFA, saturated fatty acid.

doi: 10.1111/j.1349-7006.2008.00986.x

water were available ad libitum for 9 weeks. The animals were observed daily for clinical signs and mortality, and bodyweights and food consumption were measured weekly. At the time points when the mice were killed, they were anesthetized with ether and blood samples were collected from the abdominal vein. The measurement of serum lipids, triglycerides, total cholesterol, and free fatty acids was carried out as reported elsewhere.[6] Each intestinal tract was removed, filled with 10% buffered formalin, opened longitudinally, and fixed flat between sheets of filter paper in the fixative. The experiments were conducted according to the Guidelines for Animal Experiments of the Committee for Ethics of Animal Experimentation at the National Cancer Center.

Analysis of fatty acids in biomaterials. Using accelerated solvent extraction and gas–liquid chromatography, we earlier established a new analytic method for measuring fatty acids in biomaterials.[10] The following biomaterials were applied: (1) 35 μL plasma; (2) membranes (white ghosts) prepared with sodium phosphate buffer from 50 μL erythrocytes; and (3) intestinal polyps and paired normal mucosa homogenized with the same buffer from approximately 0.3–0.5 mg formalin-fixed sample. In short, using the ASE 200 accelerated solvent extractor (Nippon Dionex, Osaka, Japan), lipids (first extraction) and fatty acid methyl esters (second extraction) were extracted with chloroform : methanol (1:2 v/v) and petroleum ether, respectively. Heptadecanoic acid and butylate hydroxytoluene were applied as an internal standard and an antioxidant, respectively. The two extraction processes were achieved automatically with computerized programs. Hydrochloride–methanol reagent was used for conversion from the extracted lipids to fatty acids and, moreover, their subsequent methyl transformation. Under conditions described previously,[10] the fatty acid methyl esters were analyzed by Shimadzu GC-2010 gas chromatography (Shimadzu, Kyoto, Japan) on a capillary column DB-225 (J. and W. Scientific, Folsom, CA, USA), equipped with an autoinjector, an autosampler, and a flame ionization detector. Individual fatty acids were identified with commercial standards of known retention time, and then integration of each peak area was carried out with GC solution software, version 2 (Shimadzu). All laboratory staff were completely blind to study subject information during fatty acid measurement.

In line with our previous studies,[9,13] we selected the 13 fatty acids described below. Individual fatty acid levels in plasma rich in triglycerides and free fatty acids were expressed as both concentrations (mmol/L) and compositions (mol% for total fatty acid concentration). Those in erythrocytes (a half life of 120 days) rich in phospholipids were expressed as compositions (mol%) because it was very difficult to measure the concentrations (mmol/L). Based on analysis of a series of 10 samples measured within 1 day, intra-assay coefficients of variation in plasma and erythrocytes were 5.0%, except for a minor group of myristic, -linolenic, and -linolenic acids (0.5% of total fatty acids for each).[10] Inter-assay coefficients of variation were based on replicate analyses of pooled erythrocytes (a total of 100 samples) over a period of 10 days and were 5.6% (6.8% for the plasma concentration of palmitoleic acid), except for the minor group of the three fatty acids, i.e. myristic, -linolenic and -linolenic acids.[10]

Selected fatty acids and grouping. The following 13 fatty acids were identified: myristic acid, palmitic acid, palmitoleic acid, stearic acid, oleic acid, linoleic acid, -linolenic acid, -linolenic acid, dihomo- -linolenic acid, AA, EPA, docosapentaenoic acid, and DHA. Using a summed value of the selected 13 fatty acids as the denominator (i.e. total fatty acids), the following five groups of fatty acids were classified: SFA (myristic, palmitic, and stearic acids); MUFA (palmitoleic and oleic acids); total PUFA (n-6 and n-3 PUFA); n-6 PUFA (linoleic, -linolenic, and dihomo- -linolenic acids, and AA); n-3 PUFA (-linolenic acid, EPA, docosapentaenoic acid, and DHA). As indicators of membrane fluidity, the saturation index$_{n-9}$ (ratio of stearic to oleic acids) and the index$_{n-7}$ (ratio of palmitic to palmitoleic acids) were used to consider the activity of the rate-limiting delta 9 desaturases (stearoyl-CoA desaturase) that transform SFA into the corresponding MUFA.[9,13] The ratio of SFA to total PUFA was applied as an indicator of competitive incorporation of fatty acids into phospholipids in erythrocyte membranes.[9,13]

Statistical methods. Mean values and their standard errors were generated for all variables. The Wilcoxon rank sum test was used to assess the significance of differences in the means of fatty acid concentrations (mmol/L) in plasma between Min and wild-type mice, because the standard errors were much higher in the wild-type mice. The numbers of multiple intestinal polyps were also compared as a variable. The mean values (mmol/L) in plasma, moreover, were adjusted for individual bodyweights at 15 weeks of age using a linear regression model, and then compared between the two groups. Pearson's correlation coefficient (r) between the serum levels of triglycerides and the bodyweights was 0.88 ($P < 0.05$). Considering the observed colinearity of the two variables, bodyweight was not included in the model. For the values (mol%) of fatty acids in plasma and erythrocyte membranes, Student's t-test was used to assess the significance of differences between the two groups. In Min mice, the paired t-test was used for the values in intestinal polyps and the paired normal mucosa as paired samples derived from the same three mice. All statistical analyses were conducted using SAS version 9.1 (SAS Institute, Cary, NC, USA) and $P < 0.05$ was considered statistically significant.

Results

Serum lipids and numbers of intestinal polyps. Bodyweight values were not different between Min (19.98 ± 0.44 and 28.68 ± 1.15 g) and wild-type mice (19.92 ± 1.64 and 28.66 ± 1.47 g) at 6 and 15 weeks of age, respectively. Using the Wilcoxon rank sum test, serum levels of triglycerides were higher in Min mice than in wild-type mice ($P < 0.005$). After adjusting for individual bodyweights at 15 weeks of age, Min mice had higher levels of total cholesterol (2.39 ± 0.20 and 1.79 ± 0.79 mmol/L, $P < 0.05$)a nd triglycerides (1.32 ± 0.15 and 0.44 ± 0.17 mmol/L, $P < 0.005$), and lower levels of free fatty acid (0.40 ± 0.04 and 0.56 ± 0.14 mEq/L, $P < 0.05$). The numbers of intestinal polyps were 68.9 ± 4.42 in Min mice and none in their wild-type counterparts.

Fatty acid levels in plasma. The plasma concentration (mmol/L) of total fatty acids was 1.6 times higher in Min mice than in wild-type mice (6.57 ± 0.53 and 4.03 ± 1.62, $P < 0.05$). Values for SFA, palmitic acid, MUFA, and oleic acid were also higher in Min mice ($P < 0.05$ for all)(Fig. 1). That of linoleic acid was 1.9 times higher in Min mice ($P < 0.05$), and those of total PUFA and n-6 PUFA were also higher ($P < 0.05$ for both). No significant variation was found for AA value. The ratio of SFA to total PUFA was lower in Min mice (0.86 ± 0.03 and 1.31 ± 0.26, $P < 0.05$). Moreover, the value (mol%) of linoleic acid was higher in Min mice (25.8 ± 1.0 and 21.3 ± 1.9, $P < 0.05$), but no differences were observed for other fatty acids. The two saturation indices did not differ between the two groups.

Fatty acid levels in erythrocyte membranes. The values (mol%) for palmitic acid, MUFA, and oleic acid, excluding SFA, were higher in Min mice ($P < 0.05$, 0.001, and 0.001, respectively) (Fig. 2), along with the ratio of SFA to total PUFA (1.98 ± 0.06 and 1.59 ± 0.08, $P < 0.005$). However, those for total PUFA, n-6 PUFA, and AA, excluding linoleic acid, were lower ($P < 0.0005$, 0.0001, and 0.0005, respectively). The saturation index$_{n-9}$ was lower in Min mice (0.67 ± 0.03 and 0.90 ± 0.02, $P < 0.001$), b ut the index$_{n-7}$ did not vary.

Fatty acid levels in intestinal polyps and paired normal mucosa in Min mice. Values (mol%) for MUFA and oleic acid were higher in intestinal polyps ($P < 0.05$ for both), but no difference was found for SFA and palmitic acid (Fig. 3). However, those of

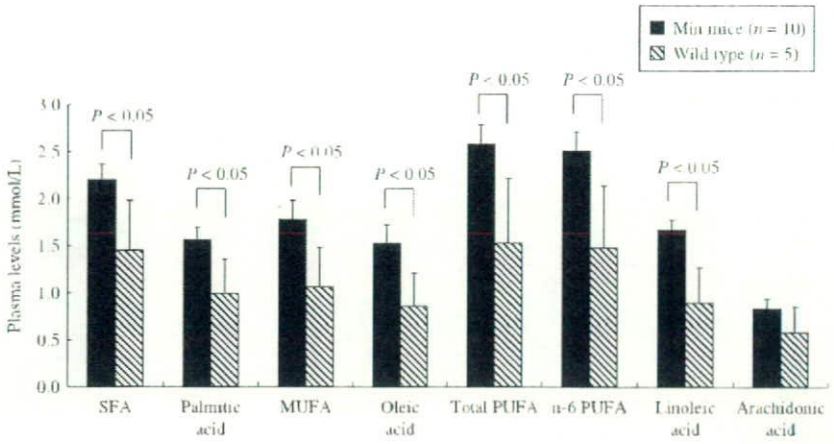

Fig. 1. Plasma levels (mmol/L) of fatty acids in Min and wild-type mice. All mice had been given an AIN-76A diet free of eicosapentaenoic and docosahexaenoic acids from 6 to 15 weeks of age. Filled and crosshatched boxes are shown for Min ($n = 10$) and wild-type ($n = 5$) m ice, respectively. Data are means; bars are standard errors. The *P*-values are shown according to a liner regression model adjusted for individual bodyweights at 15 weeks of age. MUFA, monounsaturated fatty acid; PUFA, polyunsaturated fatty acid; SFA, saturated fatty acid.

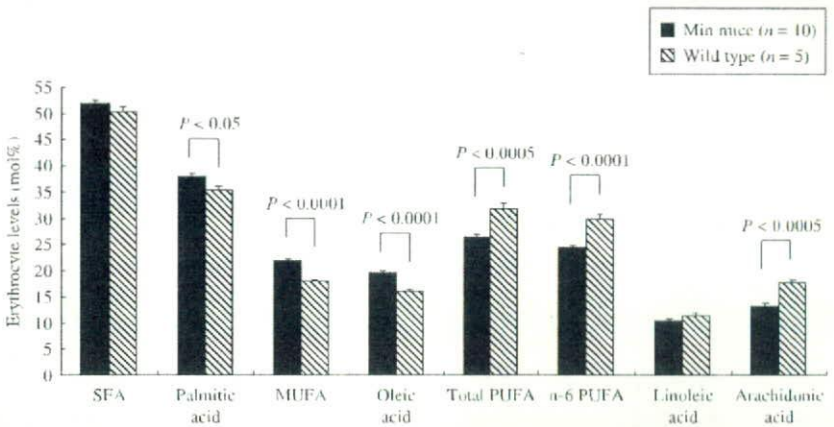

Fig. 2. Fatty acid levels (mol%) of erythrocyte membranes in Min and wild-type mice. All mice had been given an AIN-76A diet free of eicosapentaenoic and docosahexaenoic acids from 6 to 15 weeks of age. Filled and crosshatched boxes are shown for Min ($n = 10$) a nd wild-type ($n = 5$) mice, respectively. Data are means; bars are standard errors. The *P*-values for Student's *t*-test are shown. MUFA, monounsaturated fatty acid; PUFA, polyunsaturated fatty acid; SFA, saturated fatty acid.

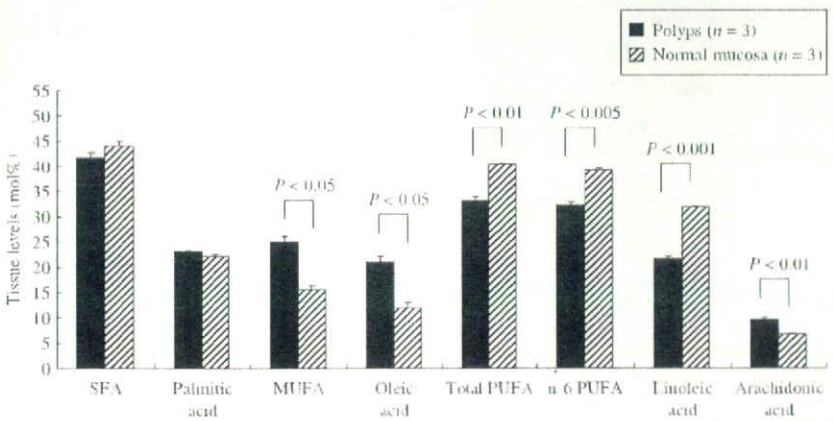

Fig. 3. Fatty acid levels (mol%) of intestinal polyps or the paired normal mucosa in Min mice. All mice had been given an AIN-76A diet free of eicosapentaenoic and docosahexaenoic acids from 6 to 15 weeks of age. Filled and crosshatched boxes are shown for intestinal polyps ($n = 3$) and the paired normal mucosa ($n = 3$) i n the same Min mice, respectively. Data are means; bars are standard errors. The *P*-values for the paired *t*-test are shown. MUFA, monounsaturated fatty acid; PUFA, polyunsaturated fatty acid; SFA, saturated fatty acid.

total PUFA, n-6 PUFA, and linoleic acid were lower in intestinal polyps ($P < 0.001$, 0.005, and 0.001, respectively), whereas the AA value was 1.43 times higher ($P < 0.01$). The ratio of SFA to total PUFA also tended to be higher in intestinal polyps (1.26 ± 0.03 and 1.09 ± 0.02, $P = 0.06$). The saturation index$_{n-9}$ was higher in intestinal polyps (1.26 ± 0.03 and 1.09 ± 0.02, $P < 0.05$), but the index$_{n-7}$ did not vary.

n-3 PUFA in the three biomaterials. Although a diet free of EPA and DHA had been fed to the mice for 9 weeks, EPA and DHA can be biosynthesized from -linolenic acid in mice *in vivo*. In plasma, the levels (both mmol/L and mol%) of n-3 PUFA and DHA had tendencies to be higher in Min mice ($P = 0.07$ for both), but -linolenic acid and EPA were not detected (Fig. 4). In erythrocyte membranes, no difference was observed for n-3 PUFA, -linolenic acid, EPA, or DHA (Fig. 4). In intestinal polyps, values for n-3 PUFA were the same as in background mucosa, but -linolenic acid tended to be lower ($P = 0.06$) (Fig. 5). Contrary to our expectations, those for EPA and DHA were 1.7–2.0 times higher in intestinal polyps ($P < 0.01$ and 0.05, respectively), corresponding to higher AA levels, but were less than one-tenth of the AA level in intestinal polyps and mucosa.

Discussion

The present study showed principal relationships between intestinal polyp formation and fatty acid levels in a series of biomaterials

doi: 10.1111/j.1349-7006.2008.00986.x

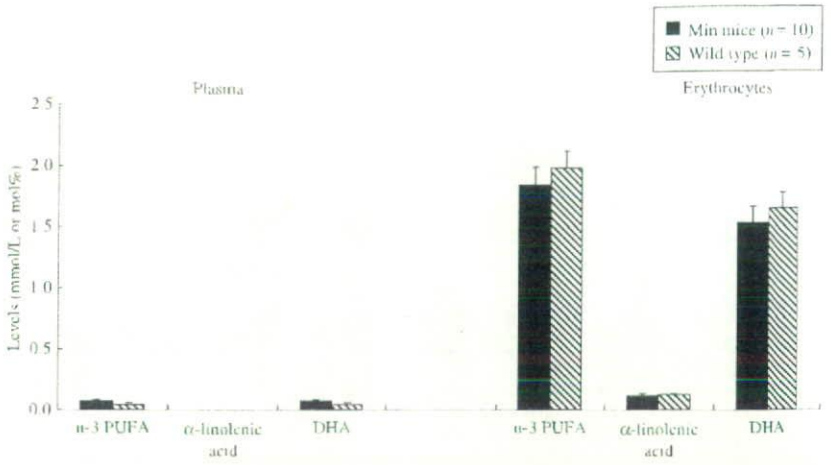

Fig. 4. n-3 Polyunsaturated fatty acid (PUFA) levels (mol%) in (left) plasma and (right) erythrocyte membranes in Min and wild-type mice. All mice had been given an AIN-76A diet free of eicosapentaenoic acid (EPA) and docosahexaenoic acid (DHA) from 6 to 15 weeks of age. EPA was not detected in plasma or trace levels in erythrocyte membranes. Filled and crosshatched boxes are shown for Min (n = 10) and wild-type (n = 5)m ice, respectively. Data are means; bars are standard errors. There were no significantly different levels for any of the variables between the two groups.

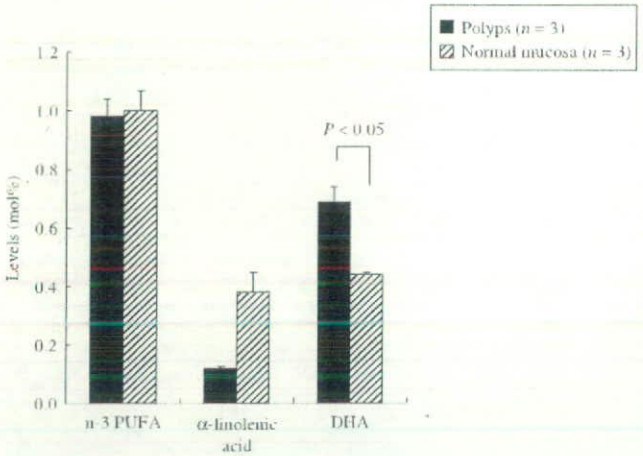

Fig. 5. n-3 Polyunsaturated fatty acid (PUFA) levels (mol%) of intestinal polyps or the paired normal mucosa in Min mice. All mice had been given an AIN-76A diet free of eicosapentaenoic acid (EPA) and docosahexaenoic acid (DHA) from 6 to 15 weeks of age. Filled and crosshatched boxes are shown for intestinal polyps (n = 3) and the paired normal mucosa (n = 3) in the same Min mice, respectively. EPA levels were trace. Data are means; bars are standard errors. The P-values for the paired t-test are shown.

(plasma, erythrocyte membranes, and intestinal polyps or the paired normal mucosa), in *Apc*-deficient Min mice fed a typical diet free of EPA and DHA. Compared with their wild-type counterparts, Min mice had higher levels of palmitic and oleic acids in plasma and erythrocytes, and higher plasma levels of linoleic acid. AA, however, was lower in erythrocytes. In Min mice, oleic acid and AA were higher in intestinal polyps than in the normal paired mucosa, but linoleic acid was lower in the polyps.

Fatty acid levels in serum, plasma, platelets, erythrocyte membranes, adipose tissue, and specific organs have been confirmed to reflect their consumption from diet and supplements, but there are both benefits and drawbacks in using these to assess impact on cancer risk.[14] First, phospholipid levels (mol%) of AA in specific organs and adipose tissue are appropriate for evaluating capacity for prostaglandin E_2 generation, but it is ethically difficult to obtain them from the general population. Second, platelets and erythrocytes are also rich in phospholipids and their fatty acid levels (mol%) are not affected by fasting or non-fasting conditions. Compared to platelets (half life 3–10 days), fatty acid levels in erythrocytes (half life 120 days) are more suitable for evaluation of dietary intake during the most recent 3 months, without recall bias. However, it is difficult to measure concentrations (mmol/L) in the solid phase. Third, most phospholipids are glycerol-3-phospahte derivatives and contain abundant SFA such as palmitic acid at the -position of glycerol, whereas both MUFA and PUFA are found predominately at the position. We showed that PUFA and SFA might compete for incorporation into phospholipids of erythrocyte membranes.[9] Forth, serum and plasma rich in triglycerides and free fatty acids should be collected under fasting conditions, and their levels (mmol/L and mol%) are less useful as measures of mid- to long-term intake.

We did not examine the roles of palmitic acid, MUFA, or oleic acid in polyp formation in Min mice, but we speculated the possible mechanisms as follows: (1) in erythrocyte membranes and intestinal polyps, the elevated levels of these fatty acids might be related to polyp formation; (2) in both biomaterials therefore the values of total PUFA and n-6 PUFA might be relatively reduces, because we showed that total PUFA and n-6 PUFA in erythrocyte membranes are negatively correlated with palmitic acid and SFA, and also with oleic acid and MUFA;[9] (3) in erythrocyte membranes, AA was also negatively correlated with palmitic acid, SFA, oleic acid and MUFA; and (4) in intestinal polyps, however, AA was selectively incorporated into the membrane phospholipids and then AA-derived metabolites, such as prostaglandin E_2, might promote polyp formation.

A literature search was undertaken of the electronic database PubMed for the years 1976–2007 (August) for publications addressing specific fatty acid levels in the three biomaterials (i.e., plasma, erythrocytes and mucosa, but not adipose tissue and feces) in relation to colorectal cancer risk. A total of 20 reports (three animal and 17 human studies) were selected.[9,15–33] Risks of sporadic colorectal cancer and FAP were summarized distinctively for relationships with fatty acid levels in plasma, erythrocytes, and intestinal mucosa (polyps or tumor tissues) in each laboratory and human study (Table 1). Our present findings are mostly consistent with previous findings for each biomaterial, excluding a report for FAP patients with and without intestinal reconstruction by colectomy.[33] In brief, colorectal cancer risk appears to be positively related to plasma values of oleic acid and erythrocyte levels of palmitic and oleic acids. Compared with their wild-type counterparts, mRNA levels for LPL have been demonstrated to be downregulated in the livers and small intestines of *Apc* gene-deficient Min and Apc^{1309} mice.[6–8,34] However, significant differences in the following mRNA levels were not observed: fatty acid synthase, stearoyl-CoA desaturase-1, acyl-CoA oxidase, carnitine palmitoyl transferase-1, and phosphoenolpyruvate carboxykinase, related to the hydrolysis of triglycerides, lipogenesis, -oxidation, and glucose homeostasis.[34]

Table 1. Relationships between risk of sporadic colorectal cancer and familial adenomatous polyposis (FAP), and fatty acid levels in plasma, erythrocyte membranes, and intestinal mucosa

		Animals[†‡]					Humans[§]			
		Sporadic colorectal cancer[†]		FAP (the present study)[‡]			Sporadic colorectal cancer			FAP
	Diet	Erythrocytes	Mucosa	Plasma	Erythrocytes	Mucosa	Plasma	Erythrocytes	Mucosa	Plasma
Individual fatty acids										
Palmitic acid	Low SFA	++[16]	– –[17]	++	++	++	NA[19]	NA[25]	NA[28]	– –[33]
	High SFA	++[16]	NA[17]					NA[26]		
	Low n-6 PUFA	++[16]	NA[18]					++[27]		
	High n-6 PUFA	NA[16]	+[18]					++[9]		
Stearic acid	Low SFA	– –	NA	NA	NA	NA	++[19]	++[25]	++[28]	– –
	High SFA	– –	NA					NA[27]	NA[29]	
	Low n-6 PUFA	NA	++					NA[9]		
	High n-6 PUFA	NA	++							
Oleic acid	Low SFA	++	NA	++	++	++	++[19]	NA[25]	NA[28]	NA
	High SFA	++	– –				NA[20]	NA[26]	++[29]	
	Low n-6 PUFA	– –	NA					++[27]		
	High n-6 PUFA	NA	NA					++[9]		
Linoleic acid	Low SFA	++	NA	++	NA	– –	– –[19]	NA[25]	NA[28]	– –
	High SFA	++	NA				++[20]	– –[26]	NA[29]	
	Low n-6 PUFA	++	– –				– –[21]	– –[27]		
	High n-6 PUFA	++	– –				NA[22]	– –[9]		
AA acid	Low SFA	– –	++	NA	– –	++	NA[19]	– –[25]	– –[21]	++
	High SFA	– –	++				NA[22]	– –[26]	++[28]	
	Low n-6 PUFA	NA	++					– –[9]	++[29]	
	High n-6 PUFA	NA	++							
EPA							– –[19]	NA[9]	– –[30]	NA
							– –[21]		– –[31]	
							NA[22]			
DHA							– –[19]	NA[21]	– –[19]	++
							–[22]	– –[9]	++[28]	
									++[29]	
									NA[30]	
									NA[31]	
Groups of fatty acids										
Total fatty acids				++						
SFA				++	NA	NA	NA[22]	++[9]		– –
MUFA				++	++	++	+[22]	NA[9]		++
TotalP UFA				++	– –	– –		– –[9]		++
n-6P UFA				++	– –	– –	NA[22]	– –[9]		NA
n-3 PUFA							–[22]	NA[9]		++
Ratios of fatty acids										
n-6 PUFAs to n-3 PUFA							– –[23]	NA[9]	NA[32]	– –
							NA[24]			
							NA[22]			
Saturation index n-9	Low SFA	NA		NA	– –	+		–[27]		++
	High SFA	NA						NA[9]		
	Low n-6 PUFA	++								
	High n-6 PUFA	NA								

+, no significant increase; ++, significant increase; –, no significant decrease; – –, significant decrease; NA, no association.
AA, arachidonic acid; EPA, eicosapentaenoic acid; DHA, docosahexaenoic acid; SFA, saturated fatty acid; MUFA, monounsaturated fatty acid; PUFA, polyunsaturated fatty acid.
[†]In laboratory studies, a series of systematically examined reports were selected considering experimental diets under the following conditions:
(1) Fatty acid levels in biomaterials were compared between two groups of mice, but not rats, treated with azoxymethane and saline (as controls).
(2) The carcinogen chemical was azoxymethane, but not 1, 2-dimethylhydrazine or others.
(3) The study endpoint was not to detect colonic aberrant crypt foci.
[‡]In the present study, plasma and erythrocyte samples in the corresponding wild-type mice (C57BL/6J) to Min mice (C57BL/6-APCMin+) were used as controls, whereas the paired normal mucosa to intestinal polyps in Min mice was defined as control.
[§]In human studies, we here updated a previous overview (1986–2002)[15] adding newly published findings. Each reference group was defined as control subjects in individual prospective cohort and case-control studies.

doi: 10.1111/j.1349-7006.2008.00986.x

Long-chain fatty acids are natural ligands of PPAR isoforms , ( ), and , and some of them have been demonstrated to play key roles in cellular differentiation, proliferation, and apoptosis induction in the colon.[35–39] As with human colonic tumors, increased expression of PPAR has been reported in the two *Apc* gene-deficient mouse strains Min and APC[309].[6] In animal studies, dose-dependent suppression of hyperlipidemia and intestinal polyp formation have been shown for bezafibrate and pioglitazone, selective PPAR and PPAR agonists that improve hyperlipidemia in both diabetic patients and animal models. PPAR is a powerful tumor-suppressor gene in the colon, and both allele losses are linked to increased sensitivity to tumor development. Such suppressor function has been proposed to depend entirely on the presence of an intact *Apc* gene. In our case-control study, moreover, a marginal positive association between SFA consumption and colorectal cancer risk was observed in subjects with the *Pro/Pro* genotype on *Pro12Ala* polymorphism of the *PPAR* gene.[40] In cancer cells, the 16-carbon SFA palmitic acid is produced predominantly by fatty acid synthase, and the inhibitor C75 has been reported to inhibit the production of prostaglandin E_2 via cyclooxyganese-independent mechanisms.[41,42] Little is known about the relationships between such fatty acids and intestinal polyp formation, but some of them may be available to use as surrogate markers.

In animals and patients with sporadic colorectal cancer and FAP, AA values in erythrocytes are consistently lowered, whereas in intestinal tissue (or polyps, adenomas, and tumors) they are evidently increased (Table 1). In the present study, our findings on AA values in erythrocytes and intestinal polyps were identical to the evidence based on a systematic literature research. Compared with the paired normal tissues, we pointed out that the AA value was significantly elevated in intestinal polyps. The mechanisms could not be clarified in the present study, but our findings are supported by increased expression of cyclooxyganese-2 and levels of prostaglandin E_2 in intestinal tumor tissue relative to those in the paired normal parts.[43–54] In other words, AA in phospholipids of normal tissues (e.g. erythrocytes) would not directly link to intestinal polyp formation. Here, we measured fatty acid levels in small samples of biomaterials using a newly developed method, which has confirmed high precision and accuracy.[10] In Min mice fed a diet free of EPA and DHA, the levels of -linoleic acid, DHA, and n-3 PUFA were very low, and EPA was not detected in the three biomaterials of Min and wild-type mice. Interestingly, we observed that the DHA level was significantly higher in intestinal polyps of Min mice, but this might be related to higher plasma levels of DHA in Min mice with hyperlipidemia.

In conclusion, the present study suggests that intestinal polyp formation is closely related to the levels of palmitic acid, oleic acid, and AA. Intriguingly, values for AA were found to be higher in intestinal polyps, but lower in erythrocyte membranes. Our data warrant further studies of fatty acids in biomaterials in Min and wild-type mice fed a diet with added EPA and DHA.

Acknowledgments and notes

The authors are grateful to the following people. Dr M.A. Moore contributed to the drafting and revising of the manuscript, and checking the English language. Ms S. Inui and Ms M. Watanabe took part in the laboratory assays. This work was supported by a Grant-in-Aid for Cancer Research for the Third-Term Comprehensive 10-Year-Strategy for Cancer Control and for Research on Advanced Medical Technology from the Ministry of Health, Labor, and Welfare of Japan. K.K. was supported by a Research Resident Fellowship from the Foundation for Promotion of Cancer Research for the Third-Term Comprehensive 10-Year-Strategy for Cancer Control during the performance of much of this work. In the present study, we declare no conflicts of interest. An application for a patent for the method to quantitatively measure fatty acids in biomaterials has been made (Japanese Patent application no. 2005-080461).

References

1 World Cancer Research Fund/American Institute for Cancer Research. *Food, Nutrition and the Prevention of Cancer: a Global Perspective*. Washington DC: American Institute for Cancer Research, 1997.
2 Kono S, Ikeda N, Yanai F, Yamamoto M, Shigematsu T. Serum lipids and colorectal adenoma among male self-defence officials in northern Kyushu, Japan. *Int J Epidemiol* 1990; **19**: 274–8.
3 McKeown-Eyssen G. Epidemiology of colorectal cancer revisited: are serum triglycerides and/or plasma glucose associated with risk? *Cancer Epidemiol Biomarkers Prev* 1994; **3**: 687–95.
4 Otani T, Iwasaki M, Ikeda S *et al.* Serum triglycerides and colorectal adenoma in a case-control study among cancer screening examinees (Japan). *Cancer Causes Control* 2006; **17**: 1245–52.
5 Mutoh M, Akasu T, Takahashi M *et al.* Possible involvement of hyperlipidemia in increasing risk of colorectal tumor development in human familial adenomatous polyposis. *Jpn J Clin Oncol* 2006; **36**: 166–71.
6 Niho N, Takahashi M, Kitamura T *et al.* Concomitant suppression of hyperlipidemia and intestinal polyp formation in Apc-deficient mice by peroxisome proliferator-activated receptor ligands. *Cancer Res* 2003; **63**: 6090–5.
7 Niho N, Takahashi M, Shoji Y *et al.* Dose-dependent suppression of hyperlipidemia and intestinal polyp formation in Min mice by pioglitazone, a PPAR ligand. *Cancer Sci* 2003; **94**: 960–4.
8 Niho N, Mutoh M, Takahashi M, Tsutsumi K, Sugimura T, Wakabayashi K. Concurrent suppression of hyperlipidemia and intestinal polyp formation by NO-1886, increasing lipoprotein lipase activity in Min mice. *Proc Natl Acad Sci USA* 2005; **102**: 2970–4.
9 Kuriki K, Wakai K, Hirose K *et al.* Risk of colorectal cancer is linked to erythrocyte compositions of fatty acids as biomarkers for dietary intakes of fish, fat and fatty acids. *Cancer Epidemiol Biomarkers Prev* 2006; **15**: 1791–8.
10 Kuriki K, Tajima K, Tokudome S. Accelerated solvent extraction for quantitative measurement of fatty acids in plasma and erythrocytes. *Lipids* 2006; **41**: 605–14.
11 Moser AR, Pitot HC, Dove WF. A dominant mutation that predisposes to multiple intestinal neoplasia in the mouse. *Science* 1990; **247**: 322–4.
12 Mutoh M, Watanabe K, Kitamura T *et al.* Involvement of prostaglandin E receptor subtype EP (4) in colon carcinogenesis. *Cancer Res* 2002; **62**: 28–32.
13 Kuriki K, Hirose K, Wakai K *et al.* Breast cancer risk and erythrocyte compositions of n-3 highly unsaturated fatty acids in Japanese. *Int J Cancer* 2007; **121**: 377–85.
14 Hunter D. Biochemical indicators of dietary intake. In: Willett W, ed. *Nutritional Epidemiology*. New York: Oxford University Press, 1990; 186–16.
15 Nkondjock A, Shatenstein B, Maisonneuve P, Ghadirian P. Specific fatty acids and human colorectal cancer: an overview. *Cancer Detect Prev* 2003; **27**: 55–66.
16 Nicholson ML, Neoptolemos JP, Clayton HA, Talbot IC, Bell PR. Dietary and erythrocyte fatty acids in experimental colorectal carcinogenesis. *Eur J Surg Oncol* 1992; **18**: 146–51.
17 Nicholson ML, Neoptolemos JP, Clayton HA, Talbot IC, Bell PR. Increased cell membrane arachidonic acid in experimental colorectal tumours. *Gut* 1991; **32**: 413–18.
18 Nicholson ML, Neoptolemos JP, Clayton HA, Talbot IC, Bell PR. Inhibition of experimental colorectal carcinogenesis by dietary N-6 polyunsaturated fats. *Carcinogenesis* 1990; **11**: 2191–7.
19 Baro L, Hermoso JC, Nunez MC, Jimenez-Rios JA, Gil A. Abnormalities in plasma and red blood cell fatty acid profiles of patients with colorectal cancer. *Br J Cancer* 1998; **77**: 1978–83.
20 Schloss I, Kidd MS, Tichelaar HY, Young GO, O'Keefe SJ. Dietary factors associated with a low risk of colon cancer in coloured west coast fishermen. *S Afr Med J* 1997; **87**: 152–8.
21 Fernandez-Banares F, Esteve M, Navarro E *et al.* Changes of the mucosal n3 and n6 fatty acid status occur early in the colorectal adenoma–carcinoma sequence. *Gut* 1996; **38**: 254–9.
22 Kojima M, Wakai K, Tokudome S *et al.* Serum levels of polyunsaturated fatty acids and risk of colorectal cancer: a prospective study. *Am J Epidemiol* 2005; **161**: 462–71.
23 Huang YC, Jessup JM, Forse RA *et al.* n-3 fatty acids decrease colonic epithelial cell proliferation in high-risk bowel mucosa. *Lipids* 1996; **31** (Suppl): 313S–7S.
24 O'Keefe SJ, Kidd M, Espitalier-Noel G, Owira P. Rarity of colon cancer in Africans is associated with low animal product consumption, not fiber. *Am J Gastroenterol* 1999; **94**: 1373–80.

25 Neoptolemos JP, Clayton H, Heagerty AM *et al.* Dietary fat in relation to fatty acid composition of red cells and adipose tissue in colorectal cancer. *Br J Cancer* 1988; **58**: 575–9.
26 Hietanen E, Bartsch H, Bereziat JC *et al.* Diet and oxidative stress in breast, colon and prostate cancer patients: a case-control study. *Eur J Clin Nutr* 1994; **48**: 575–86.
27 Kelly SB, Miller J, Wood CB, Williamson RC, Habib NA. Erythrocyte stearic acid desaturation in patients with colorectal carcinoma. *Dis Colon Rectum* 1990; **33**: 1026–30.
28 Neoptolemos JP, Husband D, Imray C, Rowley S, Lawson N. Arachidonic acid and docosahexaenoic acid are increased in human colorectal cancer. *Gut* 1991; **32**: 278–81.
29 Hendrickse CW, Kelly RW, Radley S, Donovan IA, Keighley MR, Neoptolemos JP. Lipid peroxidation and prostaglandins in colorectal cancer. *Br J Surg* 1994; **81**: 1219–23.
30 Anti M, Marra G, Armelao F *et al.* Effect of omega-3 fatty acids on rectal mucosal cell proliferation in subjects at risk for colon cancer. *Gastroenterology* 1992; **103**: 883–91.
31 Anti M, Armelao F, Marra G *et al.* Effects of different doses of fish oil on rectal cell proliferation in patients with sporadic colonic adenomas. *Gastroenterology* 1994; **107**: 1709–18.
32 Bartram HP, Gostner A, Scheppach W *et al.* Effects of fish oil on rectal cell proliferation, mucosal fatty acids, and prostaglandin E2 release in healthy subjects. *Gastroenterology* 1993; **105**: 1317–22.
33 Almendingen K, Hostmark AT, Fausa O, Mosdol A, Aabakken L, Vatn MH. Familial adenomatous polyposis patients have high levels of arachidonic acid and docosahexaenoic acid and low levels of linoleic acid and alpha-linolenic acid in serum phospholipids. *Int J Cancer* 2007; **120**: 632–7.
34 Mutoh M, Niho N, Wakabayashi K. Concomitant suppression of hyperlipidemia and intestinal polyp formation by increasing lipoprotein lipase activity in Apc-deficient mice. *Biol Chem* 2006; **387**: 381–5.
35 Lefebvre AM, Chen I, Desreumaux P *et al.* Activation of the peroxisome proliferator-activated receptor gamma promotes the development of colon tumors in C57BL/6J-APCMin/+ mice. *Nat Med* 1998; **4**: 1053–7.
36 Saez E, Tontonoz P, Nelson MC *et al.* Activators of the nuclear receptor PPAR enhance colon polyp formation. *Nat Med* 1998; **4**: 1058–61.
37 Vamecq J, Latruffe N. Medical significance of peroxisome proliferator-activated receptors. *Lancet* 1999; **354**: 141–8.
38 Vanden Heuvel JP. Peroxisome proliferator-activated receptors: a critical link among fatty acids, gene expression and carcinogenesis. *J Nutr* 1999; **129** (Suppl): 75S–80S.
39 Tanaka T, Kohno H, Yoshitani S *et al.* Ligands for peroxisome proliferator-activated receptors alpha and gamma inhibit chemically induced colitis and formation of aberrant crypt foci in rats. *Cancer Res* 2001; **61**: 2424–8.
40 Kuriki K, Hirose K, Matsuo K *et al.* Meat, milk, saturated fatty acids, the Pro12Ala and C161T polymorphisms of the PPAR gene and colorectal cancer risk in Japanese. *Cancer Sci* 2006; **97**: 1226–35.
41 Kuhajda FP. Fatty acid synthase and cancer: new application of an old pathway. *Cancer Res* 2006; **66**: 5977–80.
42 Accioly MT, Pacheco P, Maya-Monteiro CM *et al.* Lipid bodies are reservoirs of cyclooxygenase-2 and sites of prostaglandin-E2 synthesis in colon cancer cells. *Cancer Res* 2008; **68**: 1732–40.
43 Yang VW, Shields JM, Hamilton SR *et al.* Size-dependent increase in prostanoid levels in adenomas of patients with familial adenomatous polyposis. *Cancer Res* 1998; **58**: 1750–3.
44 Dong M, Guda K, Nambiar PR *et al.* Inverse association between phospholipase A2 and COX-2 expression during mouse colon tumorigenesis. *Carcinogenesis* 2003; **24**: 307–15.
45 Boolbol SK, Dannenberg AJ, Chadburn A *et al.* Cyclooxygenase-2 overexpression and tumor formation are blocked by sulindac in a murine model of familial adenomatous polyposis. *Cancer Res* 1996; **56**: 2556–60.
46 DuBois RN, Radhika A, Reddy BS, Entingh AJ. Increased cyclooxygenase-2 levels in carcinogen-induced rat colonic tumors. *Gastroenterology* 1996; **110**: 1259–62.
47 Williams CS, Luongo C, Radhika A *et al.* Elevated cyclooxygenase-2 levels in Min mouse adenomas. *Gastroenterology* 1996; **111**: 1134–40.
48 Rigas B, Goldman IS, Levine L. Altered eicosanoid levels in human colon cancer. *J Lab Clin Med* 1993; **122**: 518–23.
49 Pugh S, Thomas GA. Patients with adenomatous polyps and carcinomas have increased colonic mucosal prostaglandin E2. *Gut* 1994; **35**: 675–8.
50 Eberhart CE, Coffey RJ, Radhika A, Giardiello FM, Ferrenbach S, DuBois RN. Up-regulation of cyclooxygenase 2 gene expression in human colorectal adenomas and adenocarcinomas. *Gastroenterology* 1994; **107**: 1183–8.
51 Sano H, Kawahito Y, Wilder RL *et al.* Expression of cyclooxygenase-1 and -2 in human colorectal cancer. *Cancer Res* 1995; **55**: 3785–9.
52 Giardiello FM, Spannhake EW, DuBois RN *et al.* Prostaglandin levels in human colorectal mucosa: effects of sulindac in patients with familial adenomatous polyposis. *Dig Dis Sci* 1998; **43**: 311–16.
53 Khan KN, Masferrer JL, Woerner BM, Soslow R, Koki AT. Enhanced cyclooxygenase-2 expression in sporadic and familial adenomatous polyposis of the human colon. *Scand J Gastroenterol* 2001; **36**: 865–9.
54 Mutoh M, Takahashi M, Wakabayashi K. Roles of prostanoids in colon carcinogenesis and their potential targeting for cancer chemoprevention. *Curr Pharm Des* 2006; **12**: 2375–82.

doi: 10.1111/j.1349-7006.2008.00986.x

Periodic analysis of urethane-induced pulmonary tumors in living A/J mice by respiration-gated X-ray microcomputed tomography

Yusaku Hori,[1,2] Nobuo Takasuka,[1] Michihiro Mutoh,[1] Tsukasa Kitahashi,[1] Shuji Kojima,[2] Katsumi Imaida,[3] Masahiro Suzuki,[4] Kazushi Kohara,[4] Shuji Yamamoto,[4] Noriyuki Moriyama,[4] Takashi Sugimura[1] and Keiji Wakabayashi[1,5]

[1]Cancer Prevention Basic Research Project, National Cancer Center Research Institute, 5-1-1 Tsukiji, Chuo-ku, Tokyo 104-0045; [2]Department of Radiation Biosciences, Faculty of Pharmaceutical Sciences, Tokyo University of Science, 2641 Yamazaki, Noda-shi, Chiba 278-8510; [3]Onco-Pathology, Department of Pathology and Host-Defense, Faculty of Medicine, Kagawa University, 1750-1 Ikenobe, Miki-cho, Kita-gun, Kagawa 761-0793; [4]Research Center for Cancer Prevention and Screening, National Cancer Center, 5-1-1 Tsukiji, Chuo-ku, Tokyo 104-0045, Japan

(Received March 18, 2008/Revised May 2, 2008/Accepted May 19, 2008/Online publication July 4, 2008)

X-ray microcomputed tomography (micro-CT) with a respiratory gating system is a useful non-invasive approach to evaluate lung tumor development in living animal models. Here micro-CT was applied for the detection of lung lesions induced by a single intraperitoneal injection (250 mg/kg) of urethane in male A/J mice, at 2-week intervals from 10 to 30 weeks after carcinogen exposure. In micro-CT cross sections, lung tumor images were easily distinguished from surrounding non-tumorous tissues, the smallest detected tumor being approximately 0.5 mm in diameter. All of the urethane-treated mice ($n = 15$) developed lung tumors and the number of tumors developed in each mouse was 8.6 ± 3.9. Six tumors, determined histopathologically to be adenocarcinomas, were detected, growing at different rates during the experimental period. The most aggressive carcinoma, increasing in diameter from 0.9 to 3.5 mm within 8 weeks, was a solid-type nodule with a clear tumor margin on the micro-CT imaging. Other tumors, histopathologically adenomas, grew slowly or moderately. The results provide evidence that micro-CT is a useful non-invasive imaging approach for evaluating the characteristics and growth of lung tumors in mice. (*Cancer Sci* 2008; 99: 1774–1777)

Lung cancer is the leading cause of cancer death worldwide.[1] For detecting lung cancer, X-ray fluoroscopy has been used widely in practical screening. X-ray computed tomography (CT) is also used to detect early stage lesions and to evaluate tumor progression and metastasis during clinical treatment.[2] Moreover, X-ray CT is a useful tool for monitoring lung tumor development in living animal models[3] and major efforts have been invested in developing devices for imaging the inner anatomy of small animals. As with CT for human cases, micro-CT for rodents allows evaluation of bones and other calcified changes as well as diagnosis of soft tissue changes, such as lung tumor development.[4,5] Non-invasiveness, the ability to monitor therapeutic effects, the capacity to optimize the experimental period, and a lowering in the number of animals used can all be considered advantages of this novel approach. However, there are also disadvantages in that it is difficult to make a refined evaluation in very small rodents, and the image quality is strongly affected by motion-related artifacts. Several efforts, particularly the development of a method with a respiratory gating system for obtaining sharper images, have been made to overcome these difficulties.[6–8]

Hitherto, the utility of micro-CT has been reported for detecting lung tumors in a metastatic rodent model, a *K-ras* transgenic lung cancer model, and a urethane-induced mouse lung tumor model.[5,8–10] However, in those reports the mice were scanned only once by micro-CT, and then killed for histopathological analysis of lung lesions. Full utilization of the advantages of respiration-gated micro-CT for periodic detection of sizes in lung tumors and their growth over time has not been made.

In the present study, urethane-induced tumor development was therefore monitored periodically using respiration-gated micro-CT. The results obtained indicate that tumors grow at markedly varying speeds, which may not directly reflect the histopathological findings after autopsy. The necessity for appropriate scanning methods of micro-CT images, which link to histopathology, is discussed in the text.

Materials and Methods

Animals. Male A/J Jms Slc mice (5 weeks old) were purchased from Japan SLC (Hamamatsu, Japan). They were housed five to a plastic cage with woodchip bedding in an airconditioned animal room maintained at 24 ± 2°C and 60 ± 5% relative humidity with a 12:12 h L : D cycle. Basal diet (CE-2; CLEA, Tokyo, Japan) and water were available *ad libitum* throughout the experiment.

Treatment. The experimental protocol is shown in Figure 1. At 6 weeks of age, mice ($n = 15$) were treated with a single intraperitoneal injection of urethane (250 mg/kg; Sigma, St Louis, MO, USA) in 0.9% NaCl saline. Control mice ($n = 10$) were given a single saline intraperitoneal injection. The mice were scanned by micro-CT every 2 weeks from 10 to 30 weeks after urethane or control vehicle injection. The experiments were conducted according to the Guidelines for Animal Experiments in National Cancer Center of the Committee for Ethics of Animal Experimentation.

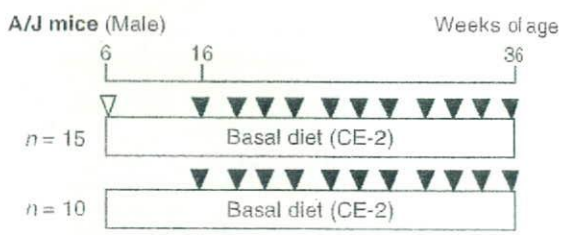

Fig. 1. Experimental protocol. Six-week-old male A/J mice were injected with 250 mg/kg urethane and killed 30 weeks later. During the experimental period, the mice were scanned by microcomputed tomography every 2 weeks from 10 to 30 weeks after urethane injection. ▽, intraperitoneal urethane; ▼, computed tomography scan.

[5]To whom correspondence should be addressed. E-mail: kwakabay@ncc.go.jp

doi: 10.1111/j.1349-7006.2008.00889.x

Table 1. Incidence and multiplicity of lung tumors in A/J mice assessed by microcomputed tomography

Treatment	No. mice	Total tumors detected at 16 weeks		Total tumors detected at 36 weeks	
		Incidence	No. tumors/mouse	Incidence	No. tumors/mouse
Urethane	15	10 (67)	1.6 ± 1.0	15 (100)	8.6 ± 3.9
Vehicle	10	0 (0)	0	0 (0)	0

Data are means ± SD. Numbers in parentheses are the percentages of mice with lung tumors.

Table 2. Incidence and multiplicity of lung tumors in A/J mice assessed histopathologically

Treatment	No. mice	Adenoma		Adenocarcinoma		Total tumors	
		Incidence	No. tumors/mouse	Incidence	No. tumors/mouse	Incidence	No. tumors/mouse
Urethane	15	15 (100)	7.1 ± 3.2	3 (20)	2.0 ± 1.0	15 (100)	9.5 ± 3.8
Vehicle	10	0 (0)	0	0 (0)	0	0 (0)	0

Data are means ± SD. Numbers in parentheses are the percentages of mice with lung tumors.

Micro-CT scan procedure. All mice were anesthetized with isoflurane (Dainippon Sumitomo Pharmaceutical, Osaka, Japan) and maintained anesthesia was achieved with a mixture of isoflurane and room air delivered during the scanning with micro-CT. Each mouse was placed on its back on an animal bed for micro-CT scanning and banded across the chest area, and a sensor for detecting respiration was placed on the abdomen. The X-ray scanning time point was set at 1200 ms after expiration.

For scanning, a new cone-beam micro-CT scanner (eXplore Locus; General Electric Healthcare, London, UK) was used. The scan parameters that are consistent for gated *in vivo* scan acquisitions include: 80 kV peak, 450 μA, 400 ms per frame, 0.5 degrees at the angle of increment, and 720 views. The measured in-air radiation at the isocenter was 240 mGy. Three-dimensional images obtained from axial, sagittal, coronal, and oblique micro-CT images were reconstructed using MicroView (General Electric Healthcare).

Histopathological examination. The mice were killed 30 weeks after urethane administration and the major organs, such as the liver, kidneys, and spleen, were weighed before fixation in 10% buffered formalin. The lungs were inflated for this purpose and lung tumors, detected using a stereoscopic microscope, were embedded in paraffin blocks and sectioned at 3 μm for placement on slides and staining with hematoxylin–eosin for histopathological evaluation. Lung lesions were diagnosed according to the criteria of the *International Classification of Rodent Tumors: Mouse*.[11]

Results

In the micro-CT images, the lung tumors were clearly distinguished from the surrounding non-tumorous tissues. Moreover, reconstructed three-dimensional images easily differentiated the tumors (globular) and blood vessels (tube structure) in the lungs, even though both have a similar X-ray absorption.

The total numbers of lung tumors detected by micro-CT are summarized in Table 1. The smallest detectable tumor was approximately 0.5 mm in diameter and the largest tumor measured 3.5 mm. At 16 weeks, that is 10 weeks after urethane injection, the incidence of tumors detected by micro-CT was 67%, and the number of tumors per mouse detected by micro-CT was 1.6 ± 1.0. The incidence of tumors increased to 100% at the end of the experiment at 36 weeks, with the multiplicity increasing to 8.6 ± 3.9 (Table 1). Table 2 shows the incidence and multiplicity of lung tumors at 36 weeks as determined by histopathological analysis. The incidence of adenoma was 100% and that of adenocarcimoma was 20%, and the numbers of adenomas and adenocarcinomas were 7.1 ± 3.2 and 2.0 ± 1.0 per mouse, respectively.

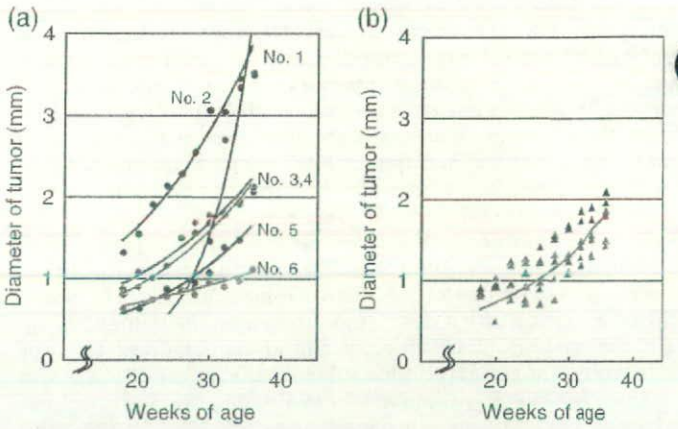

Fig. 2. Increase in pulmonary tumor diameters in A/J mice treated with urethane. (a) Growth curves of six adenocarcinomas (no. 1–6). (b) Growth curves of six representative adenomas. Each tumor scanned by microcomputed tomography was reconstructed to three-dimensional images (axial, sagittal, coronal, and oblique) and maximum diameters were measured periodically.

Figure 2a shows growth curves for all six adenocarcinomas that developed in A/J mice with urethane treatment. One tumor (no. 1) grew particularly rapidly and its diameter increased from 0.9 to 3.5 mm within 8 weeks. This solid-type nodule with a clear tumor margin on CT images is illustrated in Figure 3a–c. The earliest-detected adenocarcinoma (no. 2) grew at a moderate speed from 1.3 to 3.5 mm over 20 weeks, and was solid type with spiked edges on CT (Fig. 3d–f).

Figure 2b shows growth curves for six adenomas that developed in A/J mice with urethane treatment. The diameters of the tumors doubled at the end of the experiment, and the growth speed was almost the same as that of the adenocarcinomas (no. 3–5) shown in Figure 2a. These tumors, which grew moderately, showed clear tumor edges and/or spiked edges in a CT image (Fig. 3g–i). These lung lesions were diagnosed as bronchiolo-alveolar adenomas.

The most rapidly growing tumor (Fig. 2a, no. 1) was histopathologically diagnosed as an adenocarcinoma with poorly differentiated features (Fig. 4a,b), a solid growth pattern without

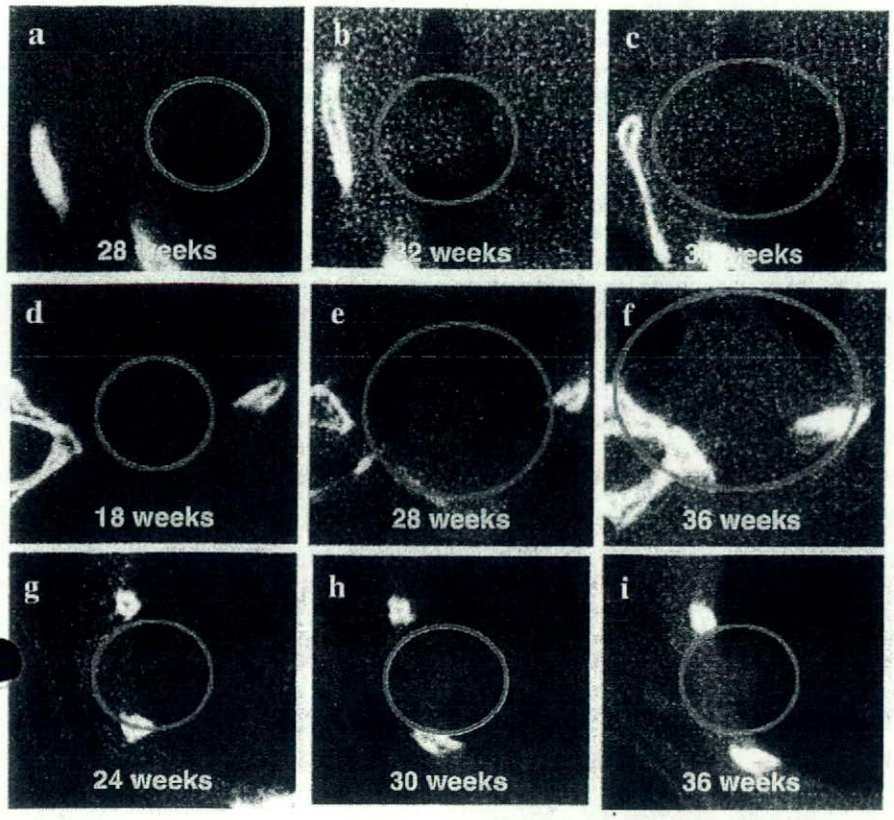

Fig. 3. Virtual *in vivo* microcomputed tomography (micro-CT) images of growing lung tumors. Axial micro-CT images of the thorax of a mouse at the indicated time points are shown. (a–c) The most aggressive lung adenocarcinoma is represented by curve no. 1 in Figure 2a. Micro-CT images, scanned at 28, 32, and 36 weeks of age, are shown. (d–f) The earliest detected lung adenocarcinoma is represented by curve no. 2 in Figure 2a. Micro-CT images, scanned at 18, 28, and 36 weeks of age, are shown. (g–i) One lung adenoma represented by a solid line is shown in Figure 2b. Micro-CT images, scanned at 24, 30, and 36 weeks of age, are shown. Tumors observed in the lung are circled.

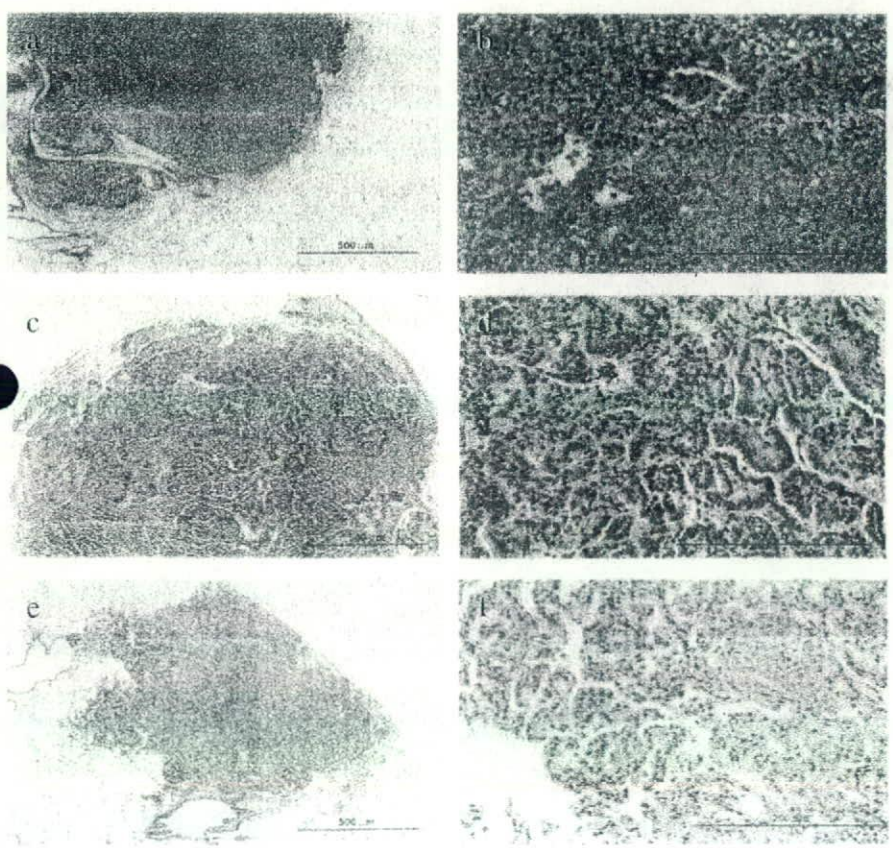

Fig. 4. Histopathological findings for lung tumors developed by urethane treatment. (a,b) The most aggressive lung adenocarcinoma is represented by curve no. 1 in Figure 2a,c,d. The earliest detected lung adenocarcinoma is represented by curve no. 2 in Figure 2a,e,f. One of the lung adenomas represented by a solid line is shown in Figure 2b. (a,c,e) Scale bar = 500 μm; magnification, ×100. (b,d,f) Scale bar = 200 μm; magnification, ×400.

doi: 10.1111/j.1349-7006.2008.00889.x

any glandular or tubular formation, and densely grouped cells with little connective tissue. Nuclei were pleomorphic with condensed chromatin. Mitotic cells were also observed frequently. Histopathology revealed all moderately growing malignancies (no. 2–4) to be adenocarcinomas with papillary formation, even though size differences were obvious between no.2 (Fig. 4c,d) and no. 3–5 (data not shown). The tumor cells had abundant eosinophilic cytoplasm, round to oval-shaped nuclei, and occasional condensed chromatin. The histopathology findings for one slow-growing tumor (no. 6) were 'carcinoma in adenoma'. Figure 4e,f illustrates a papillary-type adenoma. As seen in adenoma, few mitotic cells were observed, its nucleus was oval to round in shape, and condensed chromatin was not observed.

Discussion

In the present study, micro-CT with a respiratory gating system was shown to be useful for evaluating the developmental course of carcinogen-induced lung tumors in mouse models without invasive techniques. We used urethane-induced A/J mouse lung tumor models, because urethane has been applied as a carcinogen for mouse lung tumorigenesis studies for over 60 years and many details have been published.[12] The sensitivity of the A/J mouse is reflected in the occurrence of *K-ras* mutations in lung tumor tissue.[13] Micro-CT images here revealed that the numbers of tumors increased after urethane treatment, but that individual lesions grew differently, with the variation related mainly to histopathological features.

When counting the tumors in lung histopathological sections collected from 36-week-old mice, we found that the total number of tumors in the CT images was slightly lower than that detected by macroscopic study (8.6 per mouse vs 9.5 per mouse). It is likely that lesions in the hilus of the lung or at the periphery might be overlooked and that cardiac motion may also hinder clear imaging.

The smallest tumor detected in the present study was approximately 0.5 mm, consistent with an earlier report.[6] Although the estimated smallest size documented in the literature is 0.2 mm,[5] this was beyond the capacity in living and breathing mice even using a respiratory gating system.

The characterization of early nodules by CT imaging would help to distinguish slow-growing tumors from those growing rapidly. Characteristic micro-CT images may be observed in the shape of tumor edge and inner pattern, but in the present study the image could not show the detail of tumor development. Thus, further improvements in scanning technology are necessary to enable higher-resolution imaging to discern the differences and characteristics of early lesions and lung tumors. Moreover, it is hoped that a clear distinction between adenoma and adenocarcinoma, which grow at similar speeds, can be made by micro-CT imaging. However, at present it is also not possible to discriminate adenomas and carcinomas by micro-CT imaging. It is assumed that technical innovations may overcome these problems in the near future.

In experiments using radiography, the effects of radiation exposure (each exposure was 240 mGy) on tumor development, which could influence the outcome of the experiment, are difficult to eliminate. During our experiment, the control radiation exposure group did not develop lung tumors (Table 1). Moreover, changes in the pulmonary epithelium in response to irradiation, such as cytomegaly, multinucleation, macronucleoli, and cytoplasmic vacuolization, were not observed in either tumorous or non-tumorous lung tissues of mice treated with urethane. Further experiments are needed to clarify the effects of the amount and frequency of radiation exposure on lung tissue. To decrease the level of exposure, we limited the number of views and used half-scan mode, but further improvement in the devices is to be expected.

In conclusion, our results provide evidence that respiratory-gated micro-CT scanning of live mice has potential as a method for evaluating the growth of lung tumors. Micro-CT has the advantage of being highly sensitive compared to ultrasonography and magnetic resonance imaging in *in vivo* lung carcinogenesis experiments. In the case of magnetic resonance imaging, it produces high soft-tissue contrast, but takes time to scan the whole animal image. Moreover, a new technology may synergize two imaging methodologies, such as positron emission tomography and CT, for better assessment. This novel approach in the present study may also have an impact on the study of natural lung tumor progression or regression and cancer chemopreventive and therapeutic agents.

Acknowledgments

This work was supported by Grants-in-Aid for Cancer Research, for the Third-Term Comprehensive 10-Year Strategy for Cancer Control from the Ministry of Health, Labour, and Welfare of Japan. Dr Tsukasa Kitahashi and Dr Shuji Yamamoto were the recipients of a Research Resident fellowship from the Foundation for Promotion of Cancer Research during the time of this research.

References

1 Jemal A, Murray T, Ward E *et al.* Cancer statistics 2005. *CA Cancer J Clin* 2005; **55**: 10–30.
2 Mulshine JL. Screening for lung cancer: in pursuit of pre-metastatic disease. *Nat Rev Cancer* 2003; **3**: 65–73.
3 Paulus MJ, Gleason SS, Kennel SJ, Hunsicker PR, Johnson DK. High resolution X-ray computed tomography: an emerging tool for small animal cancer research. *Neoplasia* 2000; **2**: 62–70.
4 Kuhn JL, Goldstein SA, Feldkamp LA, Goulet RW, Jesion G. Evaluation of a microcomputed tomography system to study trabecular bone structure. *J Orthop Res* 1990; **8**: 833–42.
5 De Clerck NM, Meurrens K, Weiler H *et al.* High-resolution X-ray microtomography for the detection of lung tumors in living mice. *Neoplasia* 2004; **6**: 374–9.
6 Cavanaugh D, Johnson E, Price RE, Kurie J, Travis EL, Cody DD. *In vivo* respiratory-gated micro-CT imaging in small-animal oncology models. *Mol Imaging* 2004; **3**: 55–62.
7 Badea C, Hedlund LW, Johnson GA. Micro-CT with respiratory and cardiac gating. *Med Phys* 2004; **31**: 3324–9.
8 Cody DD, Nelson CL, Bradley WM *et al.* Murine lung tumor measurement using respiratory-gated micro-computed tomography. *Invest Radiol* 2005; **40**: 263–9.
9 Li XF, Zanzonico P, Ling CC, O'Donoghue J. Visualization of experimental lung and bone metastases in live nude mice by X-ray micro-computed tomography. *Technol Cancer Res Treat* 2006; **5**: 147–55.
10 Winkelmann CT, Figueroa SD, Rold TL, Volkert WA, Hoffman TJ. Microimaging characterization of a B16-F10 melanoma metastasis mouse model. *Mol Imaging* 2006; **5**: 105–14.
11 Ulrich M. *International Classification of Rodent Tumors: Mouse.* New York: Springer-Verlag, 2001.
12 Nettleship A, Henshaw P, Meyer H. Induction of pulmonary tumors in mice with ethyl carbamate (urethane). *J Natl Cancer Inst* 1943; **4**: 309–19.
13 Lin L, Festing MF, Devereux TR *et al.* Additional evidence that the K-ras protooncogene is a candidate for the major mouse pulmonary adenoma susceptibility (Pas-1) gene. *Exp Lung Res* 1998; **24**: 481–97.